Cross Sections for Electron Collisions with NO, N_2O, and NO_2

Cite as: J. Phys. Chem. Ref. Data **48**, 043104 (2019); https://doi.org/10.1063/1.5114722
Submitted: 11 June 2019 . Accepted: 22 October 2019 . Published Online: 31 December 2019

Mi-Young Song, Jung-Sik Yoon, Hyuck Cho, Grzegorz P. Karwasz, Viatcheslav Kokoouline, Yoshiharu Nakamura, and Jonathan Tennyson

Journal of Physical and Chemical Reference Data ARTICLE scitation.org/journal/jpr

Cross Sections for Electron Collisions with NO, N_2O, and NO_2

Cite as: J. Phys. Chem. Ref. Data 48, 043104 (2019); doi: 10.1063/1.5114722
Submitted: 11 June 2019 • Accepted: 22 October 2019 •
Published Online: 31 December 2019

View Online Export Citation CrossMark

Mi-Young Song,[1,a] Jung-Sik Yoon,[1] Hyuck Cho,[2] Grzegorz P. Karwasz,[3] Viatcheslav Kokoouline,[4] Yoshiharu Nakamura,[5] and Jonathan Tennyson[6]

AFFILIATIONS

[1]Plasma Technology Research Center, National Fusion Research Institute, 814-2, Osikdo-dong, Gunsan, Jeollabuk-do 54004, South Korea
[2]Department of Physics, Chungnam National University, Daejeon 34134, South Korea
[3]Faculty of Physics, Astronomy and Applied Informatics, University Nicolaus Copernicus, Grudziadzka 5, 87-100 Toruń, Poland
[4]Department of Physics, University of Central Florida, Orlando, Florida 32816, USA
[5]Faculty of Science and Technology, Keio University (Retired), 3-14-1 Hiyoshi, Yokohama 223-8522, Japan
[6]Department of Physics and Astronomy, University College London, Gower Street, London WC1E 6BT, United Kingdom

[a)]**Author to whom correspondence should be addressed:** mysong@nfri.re.kr

ABSTRACT

Cross section data are compiled from the literature for electron collisions with oxides of nitrogen (N_xO_y) molecules: the species nitric oxide (NO), nitrous oxide (N_2O), and nitrogen dioxide (NO_2) are explicitly considered. Cross sections are collected and reviewed for total scattering, elastic scattering, momentum transfer, excitations of rotational, vibrational, and electronic states, dissociation, ionization, and dissociative attachment. For each of these processes, the recommended values of the cross sections are presented. The literature has been surveyed up to the end of 2017. These results are supplemented by a reanalysis of the swarm measurements for NO and newly calculated cross sections for rotational excitation of N_2O and for rotational excitation and electronic excitation of NO_2.

Published by AIP Publishing on behalf of the National Institute of Standards and Technology. https://doi.org/10.1063/1.5114722

Key words: electron collisions; N_2O; NO_2; NO; Cross section; elastic scattering; momentum transfer; ionization; excitation.

CONTENTS

List of Tables

List of Figures

Published by AIP Publishing on behalf of the National Institute of Standards and Technology.

1. Introduction

Nitrogen oxides (N_xO_y) are easily generated in atmospheric plasma using N_2 and O_2 gases. Nitrogen oxides are regulated as corrosive substances and research on how to remove them is becoming of increasing importance. In our atmosphere, nitrogen oxides are generated as a byproduct of the combustion of fossil fuels, and most of them are unstable, so they are present in the atmosphere in very small amounts, meaning it can be difficult to detect their presence. The impact on the environment is almost negligible. However, two nitrogen compounds that have a great effect on the environment are NO and NO_2. NO accounts for about 95% of the nitrogen oxides generated in the combustion of fossil fuels and mostly undergoes rapid oxidization to NO_2 that is harmful to both the human body and the natural environment. N_2O is not created in the combustion of fossil fuels but is known to be generated in selective catalytic reduction (SCR) reactions and is a known cause of global warming. This paper follows our previous compilations of electron collision data for methane,[1] acetylene,[2] and NF_3.[3] It presents recommendations for electron collision cross section with nitric oxide (NO), nitrous oxide (N_2O), and nitrogen dioxide (NO_2). For a number of important processes, we were unable to identify reliable cross sections; recommendations for future work are presented in the conclusion.

All three species considered possess permanent electric dipole moments; these have important consequences for the electron collision cross sections.[4] Table 1 summarizes the key properties of NO, N_2O, and NO_2: their electric dipole moments, polarizabilities, and electron affinities. We note that Hargreaves *et al.*[5] have recently provided a comprehensive update on the spectroscopic properties of these species.

2. NO

NO is a stable, open shell species with a $^2\Pi$ ground electronic state; it has a well characterized spectrum (see Ref. 12). Figure 1 depicts its low-lying potential energy curves. These curves comprise both Rydberg-like states that converge on the more strongly bound ground state of NO^+, as represented by the A, C, D, and B' states and the valence states of which the a, B, b, L', L, I, and G states are shown in Fig. 1.

2.1. Total scattering cross section

In spite of the importance of nitrogen oxides for atmospheric chemistry, relatively few measurements of total cross sections (TCS's) for NO have been made. Recommended TCS's were given, among others, by Karwasz *et al.*,[13] Anzai *et al.*,[14] Zecca *et al.*,[15] and Itikawa.[16] The TCS for NO was measured at 1–50 eV by Brüche[17] who used Ramsauer's type spectrometer (i.e., with a perpendicular magnetic field); at 0.03–10 eV by Zecca *et al.*[18] who used a linear configuration and the retarding-field analyzer with the energy resolution of some 30–50 meV; at 100–1400 eV by Dalba *et al.*[19] using an enlarged version of Ramsauer-type geometry; at 0.5–160 eV by Szmytkowski and Maciag,[20] at 0.4–250 eV by Szmytkowski *et al.*[21] who used an electrostatic spectrometer with about 70 meV energy resolution, and at 0.16–2 eV by Alle *et al.*[22] with a time-of-flight spectrometer with the energy resolution better than 20 meV at 0.5 eV. Above 2 eV, the matching between different sets of data[18–21] is good, within 5%. A resonant structure in TCS below 2 eV was first measured by Zecca *et al.*[18] and confirmed by Szmytkowski and Maciag.[20] Measurements of Alle *et al.*[22] showed a deep structure, with TCS varying from 16.9×10^{-16} cm^2 (at 0.296 eV) to 7.3×10^{-16} cm^2 at 0.348 eV (see Fig. 2). The resonant structure was earlier observed in vibrational excitation functions and energy loss spectra and was identified due to capturing of the incoming electron into $^3\Sigma^-$ and $^1\Delta$ states of the NO^- temporary anion.

Allan *et al.*[23,24] measured differential cross sections (DCS's) at fixed angles (135°) in the energy range 0.05–2 eV using a hemispherical spectrometer with 7 meV energy resolution. These measurements resolved transitions between the two fine structure-split $^2\Pi_{1/2}$ and $^2\Pi_{3/2}$ states (separated by 15 meV), which occur via the resonant states. The measured cross sections show sharp peaks that for the interchange of the $^2\Pi_{1/2}$ and $^2\Pi_{3/2}$ states are within the energy resolution of the apparatus. The position of these peaks corresponds to the vibrational progressions of the $^3\Sigma^-$ and $^1\Delta$ NO^- states. It turned out that the cross sections for collisions

TABLE 1. Properties of NO, N_2O, and NO_2

Property	NO	N_2O	NO_2
Dipole moment[6] (1D = 3.33×10^{-30} cm)	0.157 D	0.167 D	0.316 D
Polarizability[7] (10^{-24} cm^3)	1.698	2.998	2.910
Electron affinity (eV)	0.026 ± 0.005[8]	−0.03 ± 0.10[9]	2.273 ± 0.005[10]
Ionization potential[11] (eV)	9.264 438 ± 0.000 05	12.886	9.586 ± 0.002
Bond dissociation energy[11] [D^0_{298} (kJ/mol^{-1})]	630.57 ± 0.06	167.4 ± 0.4(O–N_2), 480.7 ± 0.4 (N–NO)	306.301 (O–NO)

Published by AIP Publishing on behalf of the National Institute of Standards and Technology.

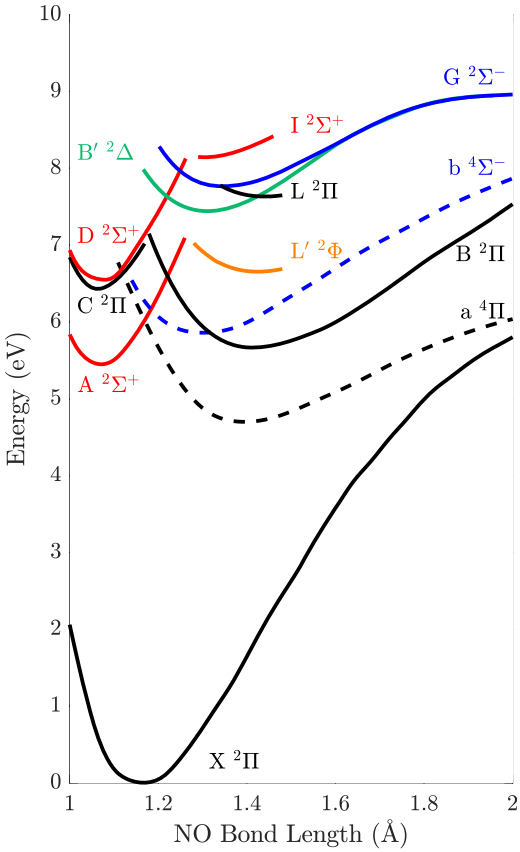

FIG. 1. Low-lying potential energy curves for NO.

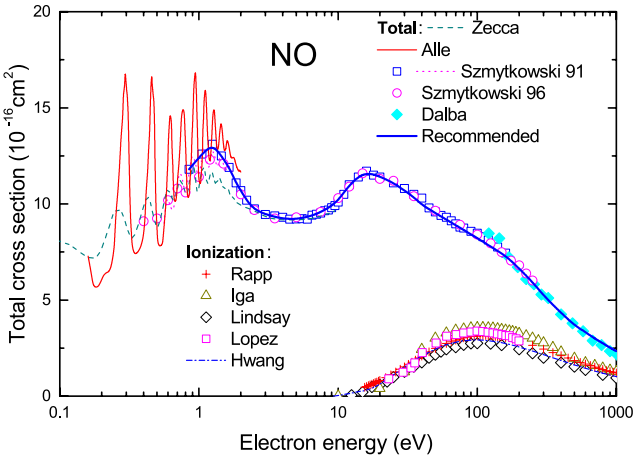

FIG. 2. TCS's for electron scattering from nitric oxide, NO. Experimental absolute TCS are from Ref. 20—squares, from Ref. 21—circles, and from Ref. 22—full curve. From Ref. 19—full diamonds; normalized data from Ref. 18—broken line; and from Ref. 20—dotted line. The thick line is for the present recommended TCS. Ionization ICS—experiments: Rapp and Englander-Golden,[28] Lindsay *et al.*,[29] Iga *et al.*,[30] and Lopez *et al.*;[31] Binary-Encounter Bethe model by Hwang *et al.*[32]

interchanging the $^2\Pi_{1/2}$ and $^2\Pi_{3/2}$ states (both inelastic $^2\Pi_{1/2} \rightarrow {}^2\Pi_{3/2}$ and super-elastic $^2\Pi_{3/2} \rightarrow {}^2\Pi_{1/2}$) are of the same magnitude (in their resonant maxima) as elastic collisions, say, of 1.3×10^{-16} cm^2/sr at 0.28–0.3 eV (see Fig. 3 in Ref. 24). Outside the resonant peaks, the measured elastic DCS (at 135°) is half of the value at the maximum. These values validate in a rough estimate (if multiplying the DCS by 4π) the TCS of Alle *et al.*,[22] within combined errors of the two experiments. In addition, the width of the resonant peaks in TCS is compatible with the 15 meV splitting and the rotational broadening of the transitions. The TCS's digitalized from the letter of Alle *et al.*[22] are given in the supplementary material of this paper. Allan's measurements of vibrational excitations[24] also showed that below 0.5 eV, the main contribution to TCS comes from the spin-orbit fine transitions, i.e., with as little as 15 meV energy loss/gain. Therefore, these transitions do not contribute significantly to the energy balance as measured in swarm experiments.[25] At energies above 200 eV, the data of Dalba *et al.*[19] from Trento are the only ones available; they were obtained with a worse angular resolution than the series of subsequent measurements from that lab.[26]

Therefore, the NO cross sections can be underestimated in their high-energy limit. In order to check it, in Fig. 3, we present the Bethe-Born (B-B) plot, where TCS in the high-energy range are approximated by the following formula:

$$\sigma(E) = A/E + B\log(E)/E. \quad (1)$$

Here, the energy is expressed in Rydbergs, Ry = 13.6 eV, and the cross sections are expressed in atomic units $a_0^2 = 0.28\times10^{-16}$ cm^2. Parameters of the fit for NO are $A = -90 \pm 10$ and $B = 370 \pm 10$. The recommended values (see Table 2 and Fig. 2) are essentially the same as in Ref. 27—above 2 eV, the mean values are from Refs. 18, 20, and 21. The uncertainty of the recommended TCS at 2–500 eV is ±5%. The recommended values above 500 eV in Ref. 27 based on the data of

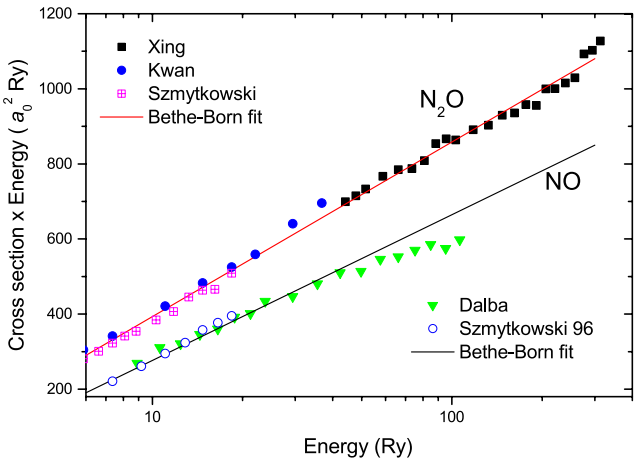

FIG. 3. Born-Bethe plot for TCS in NO and N_2O. Experimental TCS in NO are from Refs. 19 and 21; points above 500 eV from Ref. 19 are subject to the angular resolution error and, therefore, were not included in the fit. Experimental TCS's in N_2O are from Refs. 33–35. A regression line for NO_2 would coincide with that for N_2O due to much poorer quality of data (measurements of Zecca *et al.*[36] are underestimated above 1400 eV, similarly to those of Dalba *et al.* for NO).

Published by AIP Publishing on behalf of the National Institute of Standards and Technology.

Dalba *et al.*[19] have been corrected upwards to follow the B-B fit; the uncertainty is ±10%. Below 2 eV, we recommend the absolute values of Ref. 20 that are averaged over their different experimental runs, i.e., include some energy drift; therefore, these points do not show the pronounced resonant structure. These averaged values agree with the measurements of Brüche[17] done with a coarse energy resolution (no vibrational structure was seen in TCS in N_2 either, when measured by Ramsauer's method). The uncertainty of recommended values in NO below 2 eV is ±15%.

2.2. Elastic scattering cross section

Mojarrabi *et al.*[37] reported the elastic DCS of NO for the electron energy of 1.5–40 eV and for the angular range of 10°–130°. This is the only available observed DCS for the NO molecule. The numerical values are tabulated and presented in Table 3 and Fig. 4, respectively. We recommend this result for the elastic DCS of NO. However, there has been some confusion concerning the NO integral cross section (ICS). Mojarrabi *et al.*[37] reported the ICS as well as the DCS. Subsequently, Jelisavcic *et al.*[38] reported ICS for the electron energy range of 0.4–2.04 eV, which disagreed with the measurements of Mojarrabi *et al.*[37] in the overlapping energy region. Later, Brunger *et al.*[39] discovered that there had been an error made by Mojarrabi *et al.* in integrating their elastic DCS and reported a revised set of ICS's. Fujimoto and Lee[40] calculated the ICS for higher electron energies in the range 5–500 eV, using a complex optical potential consisting of static, exchange, correlation–polarization plus absorption contributions. Their result is in good agreement with the corrected result of Mojarrabi *et al.* Combining these two ICS sets, Itikawa[16] recommended the elastic ICS by joining them in the region of around 40–50 eV and estimated the uncertainty to be 25%. The recommended ICS is given in Table 4 and Fig. 5. For more detailed discussions, see Ref. 16.

2.3. Momentum transfer cross section

Itikawa[41] and Phelps[42] reported a momentum transfer cross section (MTCS) for the NO molecule, but both explained that data were uncertain and were subject to revisions. Takeuchi and Nakamura[43] also reported an elastic momentum transfer cross section determined from their electron swarm data measured in pure NO and NO-Ar mixtures, but they were not aware of the resonant character of the cross section in the low energy range and also failed to take into account the two substates of the electronic ground state of NO.

As explained in Sec. 2.2, Mojarrabi *et al.*[37] measured absolute elastic DCS and also reported momentum transfer cross section as well as the integral elastic cross section, and the latter data were later corrected by Brunger *et al.*[39] The situation for the momentum transfer cross section of Mojarrabi *et al.* also seems very much the same as in the integral elastic cross section, and therefore, their elastic DCS's are extrapolated to 0° and 180° in the manner that the resultant ICS agrees with their corrected ICS within about 2% or less and an MTCS is estimated here. Fujimoto and Lee[40] also reported theoretical elastic MTCS's for the energy range 5–500 eV. The latter two MTCS's differ between 15 and 20 eV reflecting the difference in DCS's at higher scattering angles (≥100°), as shown in Figs. 2(b) and 3(a) of Ref. 40.

One of the present authors (YN) reviewed all electron swarm data measured by Takeuchi and Nakamura[43] (see the Appendix) and determined a new set of electron collision cross sections from the revised swarm data with the help of resonant character of cross sections measured by high resolution electron beam experiments.[24,38] The elastic MTCS is determined mainly from swarm data measured in

TABLE 2. Recommended TCS (in 10^{-16} cm^2) for electron scattering on nitric oxide, NO. In the region 2–200 eV, the recommended values are based on experimental data[18–21] in relative energy overlaps. The values at 600–1000 eV are obtained from parameters of the B-B plot (see Fig. 2). The overall uncertainty of TCS is ±5% at 2–500 eV and 10% at higher energies. Below 2 eV, the recommended values are based on absolute measurements by Szmytkowski and Maciag,[20] where the resonant structure was averaged; the uncertainty is ±15%. The energy determination is 0.1 eV up to 10 eV, rising to 2 eV at 1000 eV

Electron energy	TCS	Electron energy	TCS	Electron energy	TCS
0.85	11.8	9	9.92	120	7.86
1.05	12.6	10	10.2	150	7.44
1.25	13.1	12	11.0	170	7.13
1.45	12.5	15	11.5	200	6.64
1.65	11.9	17	11.6	250	5.93
1.85	11.1	20	11.4	300	5.25
2.0	10.7	25	11.1	350	4.75
2.2	10.2	30	10.7	400	4.34
2.5	9.70	35	10.3	450	4.00
3.0	9.47	40	9.97	500	3.70
3.5	9.32	45	9.73	600	3.32
4.0	9.25	50	9.53	700	3.00
4.5	9.22	60	9.18	800	2.75
5.0	9.23	70	8.89	900	2.52
6.0	9.32	80	8.64	1000	2.34
7.0	9.48	90	8.42		
8.0	9.68	100	8.22		

Published by AIP Publishing on behalf of the National Institute of Standards and Technology.

TABLE 3. Recommended elastic DCS for NO. DCS's and uncertainties (δ) are in units of 10^{-16} cm^2 sr^{-1}

	1.5 (eV)		3.0 (eV)		5.0 (eV)		7.5 (eV)		10.0 (eV)		15.0 (eV)		20.0 (eV)		30.0 (eV)		40.0 (eV)	
Angle (deg)	DCS	δ	DCS	δ	DCS	δ	DCS	δ	DCS	δ	DCS	δ	DCS	δ	DCS	δ	DCS	δ
10															9.874	0.741		
15			0.812	0.056	0.941	0.067	1.330	0.089	1.870	0.142	3.600	0.248	4.236	0.470	6.484	0.674	6.594	0.488
20	0.799	0.057	0.850	0.055	0.949	0.062	1.234	0.083	1.629	0.109	2.907	0.282	3.444	0.468	4.490	0.489	4.364	0.319
25			0.908	0.067	1.010	0.065	1.186	0.081	1.475	0.094	2.424	0.293	2.968	0.258	3.387	0.271	3.042	0.222
30	0.843	0.056	0.942	0.069	1.095	0.070	1.202	0.079	1.375	0.088	1.922	0.185	2.132	0.171	2.290	0.195	1.958	0.143
35			0.993	0.065	1.104	0.076	1.209	0.077	1.333	0.087	1.639	0.118	1.764	0.131	1.671	0.160	1.275	0.093
40	0.910	0.062	1.028	0.066	1.121	0.077	1.221	0.087	1.292	0.084	1.409	0.094	1.502	0.188	1.323	0.147	0.885	0.066
45			1.056	0.072	1.174	0.083	1.193	0.078	1.200	0.082	1.264	0.096	1.231	0.148	0.987	0.106	0.578	0.048
50	0.955	0.063	1.081	0.071	1.148	0.074	1.207	0.082	1.172	0.076	1.109	0.095	1.036	0.112	0.739	0.112	0.410	0.033
55			1.064	0.070			1.130	0.074	1.086	0.070	0.910	0.085	0.737	0.063	0.576	0.079	0.318	0.026
60	0.960	0.068	1.074	0.073	1.114	0.072	1.067	0.070	0.996	0.071	0.739	0.062	0.567	0.045	0.417	0.046	0.245	0.018
65			1.054	0.068					0.920	0.078	0.622	0.042	0.481	0.044	0.296	0.043	0.189	0.015
70	0.947	0.063	1.004	0.066	0.976	0.063	0.873	0.059	0.752	0.052	0.529	0.034	0.361	0.034	0.249	0.040	0.149	0.012
75			0.928	0.061					0.631	0.052	0.428	0.039	0.285	0.040	0.193	0.029	0.121	0.011
80	0.895	0.059	0.864	0.058	0.802	0.052	0.647	0.045	0.517	0.037	0.343	0.039	0.233	0.026	0.157	0.031	0.101	0.008
85			0.810	0.054					0.439	0.033	0.284	0.022	0.202	0.026	0.148	0.026	0.080	0.007
90	0.838	0.058	0.742	0.057	0.642	0.042	0.496	0.033	0.373	0.027	0.278	0.021	0.186	0.019	0.138	0.017	0.070	0.006
95			0.696	0.052					0.345	0.026	0.274	0.021	0.183	0.024	0.137	0.021	0.066	0.005
100	0.805	0.052	0.622	0.042	0.534	0.034	0.409	0.027	0.333	0.021	0.305	0.023	0.197	0.021	0.136	0.017	0.068	0.006
105			0.625	0.044					0.355	0.025	0.326	0.025	0.213	0.017	0.166	0.021	0.082	0.006
110	0.774	0.053	0.597	0.045	0.472	0.031	0.395	0.025	0.366	0.025	0.382	0.025	0.246	0.024	0.206	0.021	0.110	0.009
115			0.568	0.043					0.404	0.029	0.436	0.041	0.294	0.023	0.262	0.028	0.152	0.012
120	0.761	0.053	0.538	0.034	0.443	0.028	0.421	0.027	0.448	0.031	0.472	0.035	0.326	0.037	0.315	0.058	0.206	0.020
125			0.526	0.036					0.473	0.030	0.511	0.043	0.382	0.051	0.417	0.064	0.277	0.021
130	0.750	0.049	0.517	0.035	0.441	0.029	0.470	0.031	0.519	0.035	0.536	0.040	0.454	0.062	0.498	0.093	0.345	0.030

pure NO using the vibrational excitation cross sections for NO (see Sec. 2.6) determined from swarm data measured in dilute NO–Ar mixtures almost independently of the elastic momentum transfer of NO. Because of the limited E/N range of swarm data in pure NO, the highest energy range of the derived MTCS is limited to about 40 eV. The swarm-derived elastic MTCS is shown in Fig. 6 as recommended. It merges smoothly into the theoretical one at 40–50 eV and shows the shape resonance peak at 22 eV with magnitude comparable to the

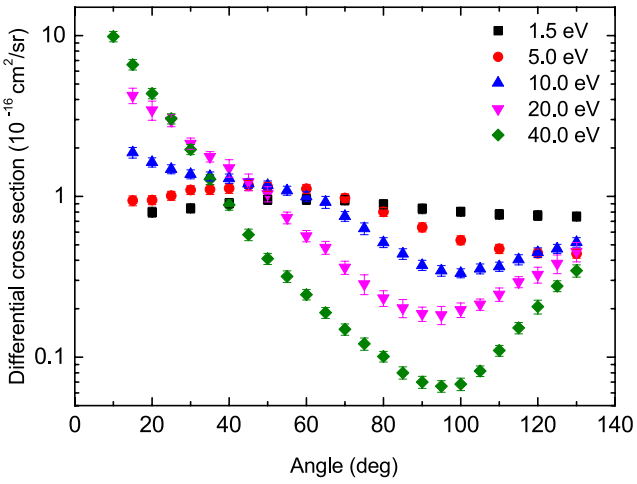

FIG. 4. Recommended elastic DCS for NO at five selected energies.

TABLE 4. Recommended elastic ICS for NO in units of 10^{-16} cm^2. Energy in eV

Energy	ICS
1.5	10.47
3.0	9.604
5.0	9.239
7.5	9.095
10	9.241
15	9.714
20	9.707
30	9.314
40	8.500
50	7.880
75	6.150
100	5.360
150	4.140
300	2.900
500	2.160

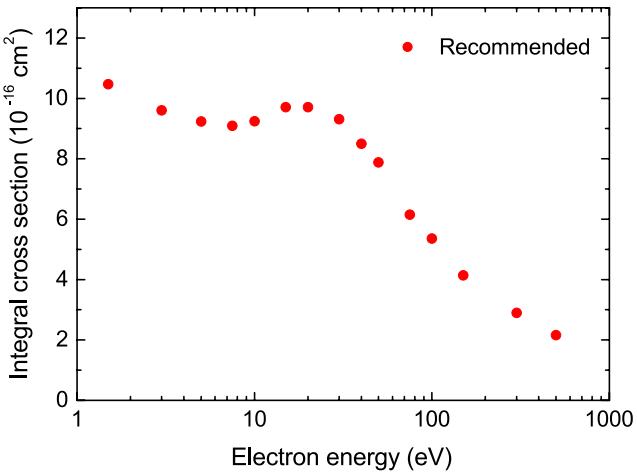

FIG. 5. Recommended elastic ICS for NO.

theory. The electron swarm method is incompetent at determining the details of the resonance structure in the lower energy range 0.1–2 eV, in principle, and must depend heavily on electron beam methods and theoretical calculations: the method can only adjust the magnitude of peaks and bottoms in a certain energy range by watching the electron energy distribution function and swarm parameters simultaneously. The result is compared with the DCS of Allan multiplied by 4π in Fig. 6. NO is polar and its elastic momentum transfer cross section increases as the incident electron energy decreases. Itikawa[41] and Phelps[42] reported larger momentum cross sections at low energy that presumably include equivalent rotational excitation cross sections (see Sec. 2.4).

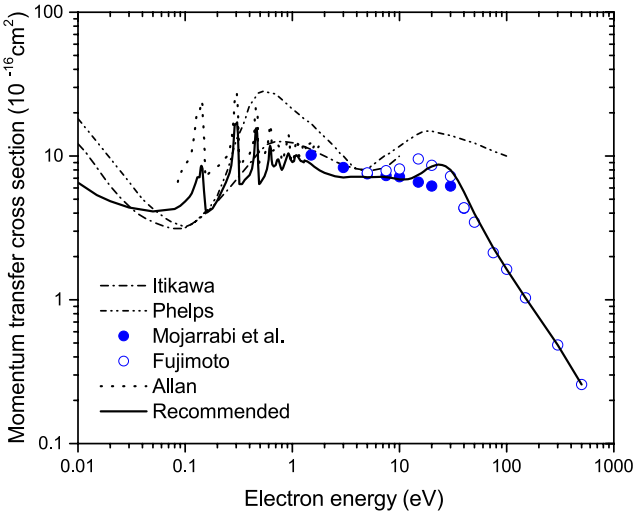

FIG. 6. Momentum transfer cross section of NO. Dashed and single dotted line, Itikawa;[41] dashed and double dotted line, Phelps;[42] solid circle, Mojarrabi *et al.*;[37] open circle, Fujimoto and Lee;[40] dotted line, Allan's[24] DCS times 4π; and solid line, recommended.

2.4. Rotational excitation cross sections

As Itikawa[16] stated in his most recent review, there is no theoretical or experimental study on rotational excitation cross sections for NO. Rotational excitation and de-excitation, however, are most effective collision processes for thermalization of slow electrons in gases through the long range interaction between electrons and molecular multipoles. The interaction is weak and the Born approximation is often employed to calculate the rotational cross sections at this low energies.[44] Rotational excitation and de-excitation cross sections given by Takayanagi[45] based on the Born approximation are used with the dipole moment of NO (0.158 D[46]) as the starting data for the present two-term Boltzmann equation analysis. The assumed gas temperature is 300 K. The energy difference of the two substates, $\Omega = 1/2$ and 3/2, of NO is only 15 meV, and at 300 K, the two states coexist in the gas with the ratio of the thermal population $\frac{n_{1/2}}{n_{3/2}} = \frac{0.64}{0.36}$. Rotational excitation and de-excitation cross sections for J up to $\Omega + 30$ were included in the Boltzmann calculation. The electron drift velocity in pure NO was measured by Takeuchi and Nakamura[47] over the E/N range 0.4–500 Td (E and N are the electric field strength and the gas number density and $E/N = 1$ Td $= 1 \times 10^{-17}$ V cm^2). The measured drift velocity changes rather monotonously with E/N on the log-log scale over the entire E/N range and the calculated one by using the Takayanagi's rotational excitation and de-excitation cross sections, on the other hand, breaks into a straight line of slope 1 at about $E/N = 0.8$ Td as decreasing E/N. The scaling factor of 0.3 or smaller is actually required in order to place the break to E/N lower than 0.4 Td. With the scaling factor of 0.3, the sum of 122 rotational cross sections, excitation and de-excitation, amounts to 8.6×10^{-16} cm^2 at electron energy 0.01 eV. Examples of the rotational excitation and de-excitation cross sections for the states corresponding to the maximum of the Boltzmann factor for 300 K, multiplied by the scaling factor 0.3, are shown in Fig. 7. Open and full circles show de-excitation and excitation cross sections, respectively, and black and colored symbols show Ω is 1/2 and 3/2, respectively.

2.5. Spin-orbit transition cross sections

As mentioned in Sec. 2.4, the $^2\Pi$ ground electronic term of NO is split into two substates. Their energy difference is only 15 meV, and their interactions with free electrons had not been studied until Allan[23] measured the electron impact cross section for the transition between them for the first time. Allan[24] also measured the absolute differential scattering cross section (see Sec. 2.2) and absolute differential inelastic ($^2\Pi_{1/2} \rightarrow {}^2\Pi_{3/2}$) and super-elastic ($^2\Pi_{3/2} \rightarrow {}^2\Pi_{1/2}$) cross sections at the scattering angle of 135°. Scattering is predominantly of resonant character, but the magnitude of the resonance peaks is almost the same as vibrational resonance, although the energy loss/gain (0.015 eV) per collision is more than an order of magnitude smaller. Assuming that both inelastic and super-elastic scattering are isotropic and the NO gas consists of the two ground electronic states at thermal equilibrium at 300 K, the equivalent set of cross sections for the spin-orbit transitions can be constructed from his experimental DCS's with scaling factors of 0.8 and 0.6 for inelastic and super-elastic scattering, respectively, as shown in Fig. 8, and this set of cross sections is confirmed to be consistent with experimental electron swarm parameters in NO[43] in the E/N range 1–10 Td through the Boltzmann equation analysis.

Published by AIP Publishing on behalf of the National Institute of Standards and Technology.

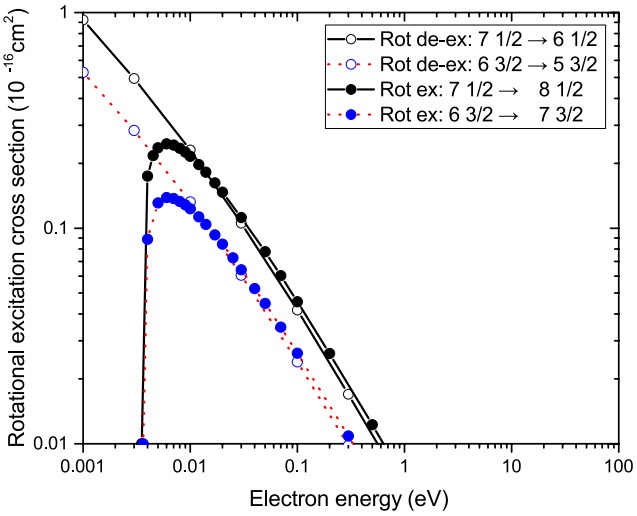

FIG. 7. An example set of rotational excitation and de-excitation cross sections at 300 K. Open and full circles show de-excitation cross section and excitation cross section, respectively. Black and colored symbols show Ω = 1/2 and 3/2, respectively.

2.6. Vibrational excitation cross sections

Mojarrabi *et al.*[37] measured absolute DCS's for vibrational (0 → 1, 2, 3, 4) excitation of the NO ground electronic state and determined integral vibrational (0 → 1, 2) cross sections in the energy range 7.5–40 eV. Allan[23] measured the detailed structure of vibrational excitation DCS's at the scattering angle 135° with high energy-resolution apparatus. Campbell *et al.*[48] constructed a set of vibrational excitation cross sections from the experimental results of Mojarrabi *et al.*[37] and Jelisavcic *et al.*[38] and also from a swarm study of Josić *et al.*[25] The numerical data of the set can be downloaded from the Flinders database at the website LXCat (www.lxcat.net).[49] Itikawa[16] recommended this set of cross sections for vibrational excitations of NO molecules. The vibrational excitation cross section data of the Flinders database were also used to re-analyze electron swarm data for NO–Ar mixtures and the analysis revealed that the set of the Flinders database needed a constant scale factor of 2 for crude agreement with the experimental results in the two NO–Ar mixtures.[47] In the course of electron swarm analysis explained in Sec. 2.3, a set of vibrational excitation cross sections consistent with the measured swarm data in pure NO and NO–Ar mixtures[47] was also derived. The results for the vibrational excitations (0 → 1, 2, 3) are shown in Fig. 9. Enhancement in energy range 1–2 eV is needed to reproduce the prominent maximum of the electron drift velocity in the 4.99% NO–Ar mixture, and a steep decrease of the cross sections in the energy range 2–3 eV and the following deep minimum ($<10^{-18}$ cm^2) up to about 7 eV are necessary for the noticeable peak structure observed in the longitudinal diffusion coefficient of electrons normalized to the gas number density, ND_L, in NO-Ar mixtures (see the Appendix). The present recommendation includes resonance reported by Mojarrabi *et al.*[37] peaked at 15 eV, but no appreciable effect from the resonance was observed in electron swarm parameters because of the overwhelming electronic excitation cross sections of NO in the overlapping energy range.

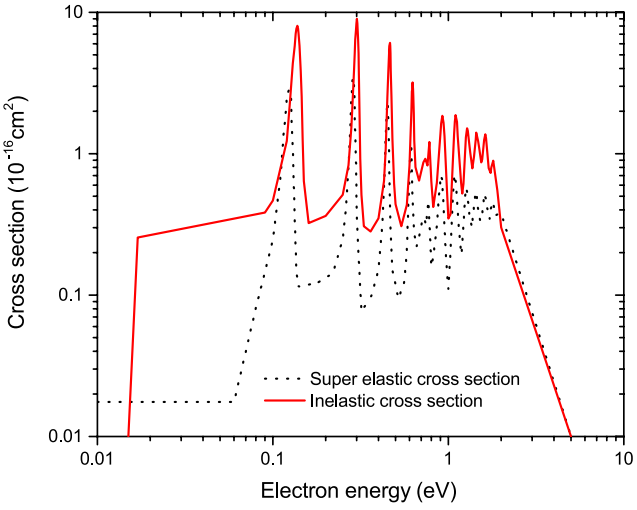

FIG. 8. Spin-orbit transition cross sections of NO at 300 K. Solid line, inelastic cross section; and dotted line, super-elastic cross section.

2.7. Electronic excitation cross section

Few measurements of electronic excitation in nitrogen oxides are available. For NO, the only complete set of differential[50] and integral[39] was given by Brunger and collaborators. Energy loss spectra at zero scattering angle, which correspond to the photoabsorption cross sections (and indicate dipole-allowed electronic excitations), were studied for all three nitrogen oxides by Brion and collaborators.[51] The photoabsorption cross sections in NO shows a rich pattern of dipole-allowed transitions with vibronic progressions (see Fig. 10).

Electronic excitation in NO was measured by Brunger *et al.*[39,50] In Ref. 50, they reported DCS's obtained from energy loss measurements at 10°–90° scattering angles and 15, 20, 30, 40, and 50 eV collision energies. The energy resolution was 35–55 meV (FWHM) and the spectra were recorded in the range 0.2–10 eV of energy loss. DCS's (for the electronic excitations) were obtained via numerical procedures from the energy loss spectra; DCS's for elastic scattering from the same group[37] were used for normalization. The estimated error was some 25% (from the uncertainty in the elastic DCS's of Mojarrabi *et al.*[37] and the analyzer response calibration) plus 5%–100% uncertainty from the numerical deconvolution of the energy loss spectra.

Brunger *et al.*[50] reported DCS for electron-impact excitation to the A $^2\Sigma^+$, E $^2\Sigma^+$, S $^2\Sigma^+$, C $^2\Pi_r$, K $^2\Pi$, Q $^2\Pi$, D $^2\Sigma^+$, M $^2\Sigma^+$, H′ $^2\Pi$, H $^2\Sigma^+$, F $^2\Delta$, and N $^2\Delta$ Rydberg electronic states; O′ $^2\Pi$ + O $^2\Sigma^+$, W $^2\Pi$ + Y $^2\Sigma^+$, T $^2\Sigma^+$ + U $^2\Delta$ + 5f, and Z$^2\Sigma^+$ + 6*dδ* + 6*f* composite Rydberg electronic states; and a $^4\Pi$, b $^4\Sigma^-$, B $^2\Pi$, L′ $^2\Phi$, B′ $^2\Delta$, and L $^2\Pi$ valence electronic states.

DCS's for dipole-allowed (Rydberg) states are forward-peaked, while for the a $^4\Pi$ and b $^4\Sigma^-$ states, they show maxima at 90° scattering angle; the type of the L′ $^2\Phi$ state is unclear: for energies 20–50 eV, the DCS is forward peaked, while at 15 eV, it resembles the DCS for dipole-forbidden states.

Published by AIP Publishing on behalf of the National Institute of Standards and Technology.

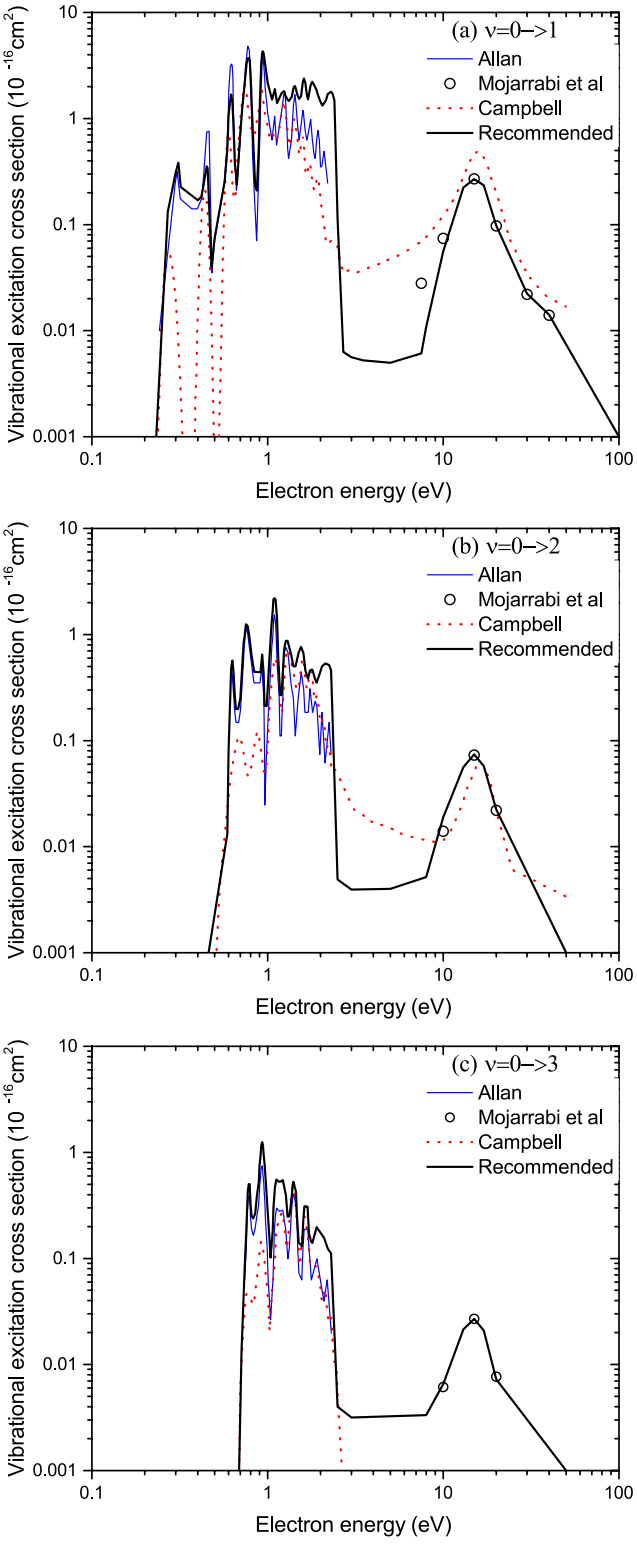

FIG. 9. Vibrational excitation cross sections for NO. Open circle, Mojarrabi *et al.*;[37] blue line, Allan's DCS times 4π; red dotted line, Campbell *et al.*;[48] Solid line, recommended.

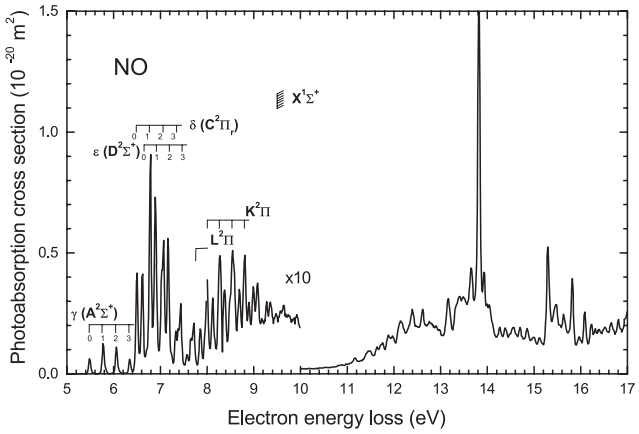

FIG. 10. Energy loss spectra in NO at 3000 eV electron collision energy and 0° scattering angle, adapted from Ref. 51.

Experimental angular dependences[50] for the A $^2\Sigma^+$, C $^2\Pi_r$, and D $^2\Sigma^+$ generally agree in shape with the theory,[52] but absolute values of the experimental DCS[50] are generally lower by a factor of two to three. Kato *et al.*[53] measured at 100 eV DCS for the A $^2\Sigma^+$, C $^2\Pi_r$, and D $^2\Sigma^+$ at forward scattering angles (4°–16°). Their DCS's at 10° are slightly (15%–20%) higher than the DCS at the same angle and 50 eV by Brunger *et al.*[50]

ICS's[39] were obtained from the DCS[50] by integration (and extrapolation to experimentally inaccessible angles). For Rydberg states, the theoretical Born scattering amplitudes were used to extrapolate to 0° scattering angle. For valence states, three techniques were used: "by eye" procedure, polynomial fits, and the molecular phase shift analysis.

ICS's for the 16 Rydberg and 6 valence states at 15–50 eV as obtained by Brunger *et al.*[39] are given in Table 5. Declared errors on these data come from both uncertainties on DCS and extrapolation procedures; they vary from 30% for the strongest excitations to 60% for the lowest.

The sum of Rydberg states shows a maximum of 0.23 $\times$ 10^{-16} cm^2 at 40 eV, while for the valence states (including the L $^2\Pi$)—a maximum of 0.3 $\times$ 10^{-16} cm^2 at 30 eV. According to the experiment,[39] the electronic excitation into the 22 states studied would amount merely to 5% of the TCS. In comparison, the difference between TCS and the sum of ionization and elastic cross sections is at 15–20 eV some 2 $\times$ 10^{-16} cm^2. Experimental ICS's grouped by the type of excitation (Rydberg and valence) and the excitation energy are shown in Fig. 11. From this figure, it is clear that excitations to the valence a $^4\Pi$ and b $^4\Sigma^-$ (excitation thresholds 4.74 eV and 5.72 eV, respectively) reach maximum at some 15–20 eV, to the valence B $^2\Pi$, L′ $^2\Phi$, and B′ $^2\Delta$ states (5.64 eV, 6.60 eV, and 7.44 eV thresholds, respectively) reach maximum at 30 eV and then drop rapidly with rising energy. Excitations to Rydberg states (and to the state identified as L $^2\Pi$) reach maxima at 40 eV (see Fig. 11).

The agreement of Brunger *et al.*'s[39] ICS's with the measurements of Skubenich *et al.*[54] is rather poor, with discrepancies up to a factor of five. The optical emission from the A $^2\Sigma^+$ state was extensively studied by Schappe *et al.*[55] up to 1000 eV collision energy. To obtain absolute values, they used normalization to the N_2 emission. They concluded

Published by AIP Publishing on behalf of the National Institute of Standards and Technology.

TABLE 5. ICS's (in 10^{-19} cm^2 units) for electron-impact excitation of the Rydberg and valence states of the nitric oxide, NO (from Ref. 39)

Rydberg state	Energy 15 (eV)	Energy 20 (eV)	Energy 30 (eV)	Energy 40 (eV)	Energy 50 (eV)
A $^2\Sigma^+$	12.23	14.83	20.15	17.59	12.33
E $^2\Sigma^+$	2.27	2.67	3.37	3.93	2.66
S $^2\Sigma^+$	4.11	8.76	15.35	10.47	6.68
C $^2\Pi_r$	23.10	32.74	41.32	46.77	32.69
K $^2\Pi$	6.73	8.09	16.29	18.90	10.32
Q $^2\Pi$	4.71	6.63	12.13	14.63	9.18
D $^2\Sigma^+$	14.40	18.53	25.37	29.68	21.99
M $^2\Sigma^+$	4.22	5.63	9.70	10.56	6.28
H′ $^2\Pi$	4.22	5.89	6.92	9.32	5.90
H $^2\Sigma^+$	5.75	8.70	13.80	13.67	8.38
F $^2\Delta$	4.40	6.07	9.29	12.82	8.00
N $^2\Delta$	2.55	-	5.30	5.84	5.64
O $^2\Pi$	4.64	6.49	15.36	13.06	8.69
W $^2\Pi$	9.43	13.40	22.70	21.74	13.36
T $^2\Sigma^+$	1.53	2.31	4.72	4.34	1.74
Z $^2\Sigma^+$	0.98	1.10	2.11	1.53	1.51
Sum	105.3	141.8	223.9	234.9	155.4
Valence state	**Energy 15 (eV)**	**Energy 20 (eV)**	**Energy 30 (eV)**	**Energy 40 (eV)**	**Energy 50 (eV)**
a $^4\Pi$	7.63	9.83	13.51	9.49	6.74
b $^4\Sigma^-$	47.12	46.53	41.37	19.64	9.40
B $^2\Pi$	11.86	14.99	21.26	14.66	12.39
L′ $^2\Phi$	27.29	22.96	18.37	21.16	20.27
B′ $^2\Delta$	32.45	65.26	84.19	57.76	21.58
L $^2\Pi$	36.06	54.68	118.5	139.26	118.5
Sum	162.4	214.3	297.2	262.0	188.9

that despite the effects of cascades, the emission cross sections from vibronic levels are proportional to the corresponding excitation cross sections. This observation yielded an absolute cross section for the excitation of the A $^2\Sigma^+$ state of 40×10^{-19} cm^2 at its maximum at 30 eV. This is a factor of two higher than the value reported by Brunger *et al.*[39] In addition, the energy dependence measured by Schappe *et al.* differs from that from Ref. 39 (see Fig. 12).

Xu *et al.*[56] determined experimentally the generalized oscillator strength (GOS) at 1500 eV collision energy for the A $^2\Sigma^+$, C $^2\Pi$ and D $^2\Sigma^+$ states and performed a detailed analysis of the results obtained with other determinations (via electron scattering, photoabsorption, lifetime, and calculations) giving the ranges of confidence. Using their GOS and Kim's[57] Born Effective (BE) scaling model, they obtained electron excitation cross sections from thresholds up to 2500 eV. For the A $^2\Sigma^+$ and C $^2\Pi$ states, the BE model agrees within experimental error bars with the measurements of Brunger *et al.* (see Fig. 12 for the A $^2\Sigma^+$ state). For the D $^2\Sigma^+$ state, the experiment[39] seems to be underestimated by a factor of 2 (Xu *et al.* corrected the data of Brunger *et al.* for vibronic populations; see their paper for details).

Olszewski and Zubek[58] studied optical emission from the A $^2\Sigma^+$ state in the threshold region. They derived ICS's for excitations to the $v = 0$ and $v = 1$ vibronic states; threshold peaks are visible for both

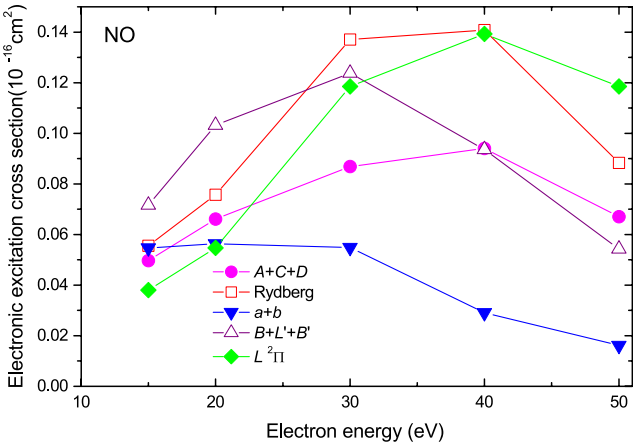

FIG. 11. Experimental[39] ICS's for electronic excitation, grouped by the type of excitation and threshold energies. Rydberg states: circles, the sum of A $^2\Sigma^+$, C $^2\Pi$, and D $^2\Sigma^+$ states (threshold energies 5.64 eV, 6.50 eV, and 6.61 eV, respectively); open squares, remaining 15 Rydberg and mixed states as measured by Brunger *et al.*,[39] starting from the E $^2\Sigma^+$ state (threshold 7.55 eV) up to the Z $^2\Sigma^+$ state (8.86 eV threshold). Valence states: inverted triangles, the sum of a $^4\Pi$ and b $^4\Sigma^-$ states (excitation thresholds 4.74 eV and 5.72 eV, respectively); open triangles, the sum of valence B $^2\Pi$, L′ $^2\Phi$, and B′ $^2\Delta$ states (5.64 eV, 6.60 eV, and 7.44 eV thresholds); diamonds, the L $^2\Pi$ state (7.76 eV threshold).

substates. Olszewski and Zubek, using the Franck-Condon factors of Brunger *et al.*,[50] suggested that the ICS for the excitation of the A $^2\Sigma^+$ state, as given by Brunger *et al.*,[50] is underestimated by a factor of three at 15 eV. Note that the measurements of Imami and Borst[59] agree with the semiempirical model of Xu,[56] giving a maximum of the emission cross section for the γ-band (i.e., the A $^2\Sigma^+$) of 0.11×10^{-16} cm^2 at 19 eV.

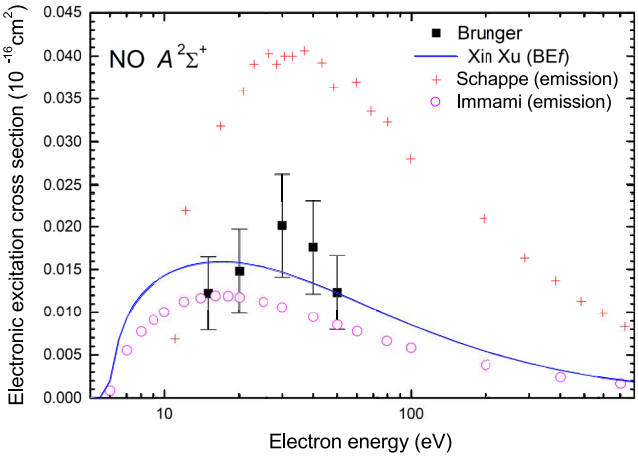

FIG. 12. ICS for the excitation into A $^2\Sigma^+$ state of nitric oxide NO. Squares, direct measurements of the electronic excitation via DCS from energy loss spectra;[39] circles and crosses, optical emission (γ-band) absolute cross sections calibrated to nitrogen emission cross sections (5 vibronic states[59] and 31 vibronic states[55]), respectively; line, BE-energy model with the generalized optical strength directly measured.[56]

Published by AIP Publishing on behalf of the National Institute of Standards and Technology.

In conclusion, we recommend for the $A^2\Sigma^+$, $C^2\Pi$, and $D^2\Sigma^+$ states, the semiempirical Born-scaled (BE) cross sections of Xu *et al.*[56] (see Table 6). These three states cover only a part of possible electronic excitation (see the energy-loss spectra in Fig. 10). Therefore, the sum of the three states would underestimate the major energy loss of drifting electrons and overestimate ionizing events in modeling electron swarms in the gas. There is another assessment of the (total) cross section for electronic excitations using an electron swarm method. Most electronic excitation thresholds of atoms and molecules lie immediately below the ionization threshold, and the electron energy losses through electronic excitations can effectively determine the overlap between the electron energy distribution function and the ionization cross section, namely, the threshold behavior of the primary ionization coefficient, one of the basic parameters in gas discharge physics. The experimental procedures for the measurement of the parameter are well established, and the claimed uncertainty of the primary ionization coefficient lies usually within a few percent range. The claimed uncertainty of experimental ionization cross section for atoms and molecules is also usually small. A trial-and-error procedure may be used to derive information about excitation cross sections from the primary ionization coefficient as a function of E/N. Electronic excitation thresholds of NO are substantially lower than those of argon atom, and electron swarm parameters in NO-argon mixtures may also be used for that purpose (see the Appendix). The resultant electronic excitation cross sections, however, should be understood as a whole only to provide realistic energy loss of electrons passing through the gas, and in fact, unique determination of individual cross sections will not be possible as long as there is no additional information. For the sum of all electronic excitation cross sections for NO, we recommend values shown in Fig. 13 in order that all electron swarm data are measured in pure NO and NO–Ar mixtures simultaneously. The present recommendation is compared with the sum of ICS's for 22 electronic excitations measured by Brunger *et al.*[50] in Fig. 13. There is about a factor of five difference between them, but the present magnitude around the peak is comparable with the difference between the present TCS and the sum of present elastic and ionization cross sections.

2.8. Dissociation cross section

Dissociation into neutral fragments was studied by LeClair *et al.*[60] who identified two channels contributing to the production of $O(^1S)$, with the kinetic energy release of 3.4 and 7 eV, but no cross sections were given. VUV emission from atomic fragments was subject to numerous studies, but the agreement between different experiments is poor (see also Ref. 61).

2.9. Ionization cross section

NO^+ ions are supposed to be responsible for a newly documented type of aurora.[62] Ionization in nitrogen oxides (NO and N_2O) was already measured in the 1930s by Tate and Smith[63] and in the 1960s by Rapp and Englander-Golden,[28] and the latter results remain

TABLE 6. Recommended cross sections for electronic excitation of NO into A $^2\Sigma^+$, C $^2\Pi$, and D $^2\Sigma^+$ states from the BE scaling model[56] in 10^{-18} cm^2 units

Energy (eV)	A $^2\Sigma^+(v = 0–3)$	C $^2\Pi(v = 0–3)$[a]	D $^2\Sigma^+$ $(v = 0–3)$[b]
5.5	0.012	0	0
6.0	0.196	0	0
6.5	0.679	0.012	0
7.0	0.934	0.591	0.352
8.0	1.20	1.65	1.12
9.0	1.34	1.97	1.59
10	1.43	2.69	1.96
12	1.53	3.31	2.51
15	1.58	3.86	3.06
20	1.58	4.28	3.56
25	1.53	4.41	3.80
30	1.47	4.39	3.89
40	1.34	4.21	3.87
50	1.23	3.97	3.75
70	1.04	3.5	3.44
100	0.853	2.96	3.01
150	0.660	2.35	2.49
200	0.542	1.96	2.13
300	0.404	1.49	1.67
400	0.325	1.21	1.38
500	0.274	1.03	1.18
700	0.21	0.794	0.919
1000	0.157	0.601	0.695

[a] b $^2\Pi(v' = 7, 10, 12)$ and L′ $^2\Phi(v' = 4)$ involved.
[b] A $^2\Sigma^+$ $(v = 4, 5, 6)$, B $^2\Pi$ $(v' = 8)$, and L′ $^2\Phi(v' = 5)$ involved.

Published by AIP Publishing on behalf of the National Institute of Standards and Technology.

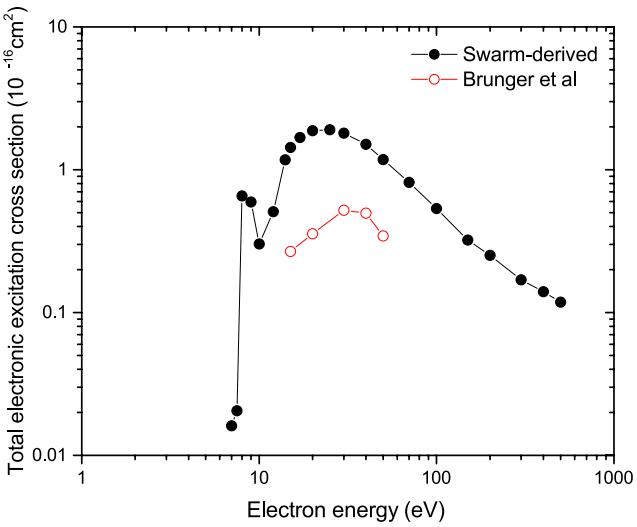

FIG. 13. The TCS for electronic excitations. Solid circle, the present total electronic excitation cross section; open circle, the sum of 22 electronic excitation cross sections measured by Brunger *et al.*[50]

still of relevance. Rapp and collaborators used a simple geometry, with gas confined in a scattering cell (i.e., with a well determined length and gas pressure), collecting the total current of ions, i.e., measuring the so-called gross total ionization cross sections. The advantage of this method is simplicity and accuracy. A disadvantage is that multiply charged ions contribute to an overestimation of the probability for an atom/molecule to be ionized (that is quantified by the counting ionization cross section) (see a detailed discussion for CH_4 by Song *et al.*[1])

However, in nitrogen oxides, the ionization into multiply charges ions is an insignificant part of the total counting ionization cross section: in NO, the cross section for the formation of the NO^{2+} is less than 2% of the total counting ionization cross section,[29] the sum of the partial cross sections for the N^{2+} ion formation and for the O^{2+} ion formation is 0.1%–0.2% of the total counting cross section,[29,64] and in N_2O, it was not measurable.[27]

Generally, the agreement between different measurements in NO is good: some systematic discrepancies are to be attributed to differences in experimental setups. The laboratory in Innsbruck used a double-focusing ion selector, with electrostatic plus magnetostatic field sectors.[65] The extraction of ions from the interaction region was performed with a weak penetrating electric field, which did not ensure collection of ions with high residual kinetic energies. In particular, cross sections for the formation of light ions, like N^+ or O^+, can be underestimated (see, for example, Fig. 14 in Ref. 66). Cross sections were obtained via normalization to Ar ionization cross sections via a relative-flow technique to determine gas density.

Iga *et al.*[30] used the method of crossed beam—electrons were intercepting the effusive gas beam at the right angle; two spectrometers—a quadrupole and a time-of-flight—were used in a complementary manner. Cross sections were normalized to those in argon. The uncertainty on absolute values[30] is ±15%.

Lindsay *et al.*[27,29] used a rather simple apparatus with a long interaction region, a time-of-flight system for extracting ions, and a position-sensitive detector to determine the recoil kinetic energy of ions. The declared accuracy of absolute values is 5% for parent ionization, rising to 30% for ions with low intensities.

Lopez *et al.*[31] used a method of crossed beams. In order to allow measurements also on radicals, they used a beam of neutral molecules, produced from a collision-induced neutralization of previously obtained positive ions. However, the exact determination of the density of the target gas beam was not straightforward and required normalization. Experimental uncertainties were ±15% on parent ionization and ±18% on dissociative ionizations.[31]

Nitrogen oxides were also one of the first molecules on which the binary-encounter B-B model[66] was applied.[32,67,68] Surprisingly, NO is the molecule for which the biggest discrepancies, up to 20%, are reported in the ionization from different laboratories. This, as already noted by Rapp and Englander-Golden[28] and quoted recently by Itikawa,[16] can be due to a high reactivity of this gas and of the ions formed. However, considering the combined error bars, the agreement is still fair (see Fig. 14).

In particular, the total counting ionization by Lindsay *et al.*[29] agrees within the error bar with the gross TCS by Rapp and Englander-Golden.[28] Counting TCS's by Lopez *et al.*[31] and by Iga *et al.*[30] are higher, but still remain within the combined error bars. Therefore, we recommend total ionization cross sections in NO by Lindsay *et al.*,[29] which also agree with the BEB model calculations of Kim and collaborators.[32] The recommended values are given in Table 7; the uncertainty in the whole energy range is ±5%.

The same considerations as above on the quality of data regard partial cross sections in NO. For the parent ion NO^+ production, the spread among different sets is some 25%, with discrepancies similar to those in the total ionization cross sections (see Fig. 15): the highest set is that by Iga *et al.*,[30] data of Kim *et al.*[66] from Innsbruck and Lopez *et al.*[31] are intermediate, and those by Lindsay *et al.*[29] are the lowest. We recommend the experimental results by Lindsay *et al.*[29] with an uncertainty of ±10%.

For fragment ions from NO, good agreement is seen between the data of Iga *et al.*[30] and Lindsay[29] for N^+, and somewhat worse for O^+

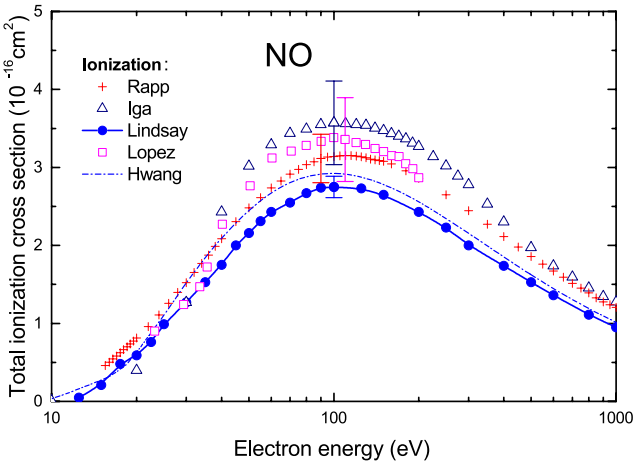

FIG. 14. Total ionization cross sections in NO: gross total—Rapp and Englander-Golden;[28] counting total—Iga *et al.*,[30] Lindsay *et al.*,[29] and Lopez *et al.*[31] Declared error bars are shown only in the maximum of the cross section. BEB model by Hwang *et al.*[32] Recommended data are those by Lindsay *et al.*[29]

Published by AIP Publishing on behalf of the National Institute of Standards and Technology.

(see full symbols in Fig. 16). For the unresolved ($N^+ + O^+ + NO^{2+}$) ionization, the results of Lopez *et al.*[31] are the highest, as they also include the NO^{2+} signal. As measured by Kim *et al.*[66] and Lindsay *et al.*,[29] this maximum for the NO^{2+} partial cross section is some 0.03×10^{-16} cm^2 (see Fig. 15).

For the reasons discussed in the description of experimental methods, for the summed ($N^+ + O^+ + NO^{2+}$) and fragment N^+, O^+ ions, we recommend the data of Lindsay *et al.*[29] with uncertainties of ±5%, ±15%, and ±20%, respectively.[29] For the double ionization NO^{2+}, we recommend data from Innsbruck[66] from threshold up to 180 eV and data from Lindsay *et al.*[29] at higher energies. The recommended total and partial cross sections in NO are shown in Fig. 17 and given in Table 7, respectively.

2.10. Electron attachment (DEA) cross section

Rapp and Briglia[69] measured the absolute TCS's for negative-ion formation in NO by electron impact in a total ionization tube. The dissociative electron attachment (DEA) channel forming this negative ion is O^- from NO. Orient and Chutjian[70] identified three channels forming $O^-(^2P)$, but did not present the absolute cross sections. Rapp and Briglia[69] is the only available measured DEA cross sections and we recommend their result as Itikawa[16] did. The recommended cross sections are presented in Table 8 and Fig. 18. Note that the units are in 10^{-18} cm^2. The uncertainty was estimated to be 10%. For detailed discussions, see Ref. 16.

TABLE 7. Recommended total and partial cross sections for electron-impact ionization of nitric oxide, NO in 10^{-16} cm^2. Energy in eV

Energy	NO^+	N^+	O^+	NO^{2+}	Total
12.5	0.048				0.048
15	0.21				0.21
17.5	0.48				0.48
20	0.59				0.59
22.5	0.75				0.76
25	0.98	0.014	0.004		0.99
30	1.20	0.054	0.013		1.27
35	1.37	0.132	0.022		1.53
40	1.51	0.191	0.046	0.000 17	1.75
45	1.67	0.252	0.073	0.001 5	2.00
50	1.74	0.317	0.104	0.004 2	2.16
55	1.84	0.315	0.140	0.007 6	2.31
60	1.89	0.375	0.158	0.011 3	2.43
70	1.92	0.444	0.170	0.015 8	2.55
80	1.96	0.479	0.199	0.025 0	2.67
90	1.97	0.481	0.251	0.029 5	2.74
100	1.97	0.506	0.247	0.029 5	2.75
125	1.92	0.499	0.286	0.032 1	2.73
150	1.84	0.502	0.274	0.029 5	2.65
200	1.69	0.438	0.267	0.030 6	2.43
250	1.55	0.406	0.246	0.028 4	2.23
300	1.40	0.385	0.191	0.023 3	2.00
400	1.24	0.309	0.168	0.023 2	1.74
500	1.11	0.265	0.139	0.020 3	1.53
600	0.98	0.228	0.139	0.014 7	1.36
800	0.81	0.190	0.100	0.013 2	1.11
1000	0.70	0.169	0.076	0.006 9	0.95

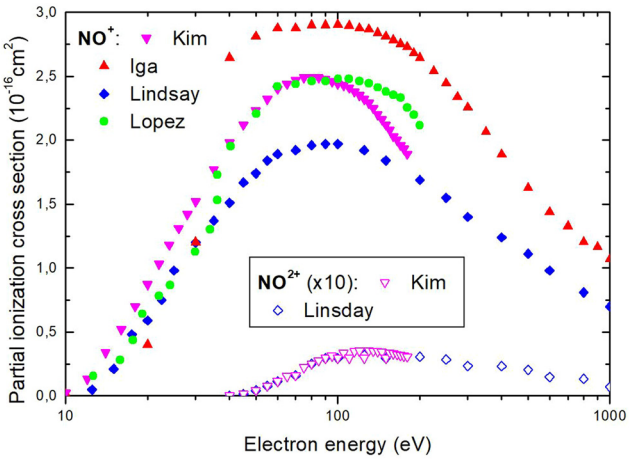

FIG. 15. Partial ionization cross sections for ionization of NO by electron impact: parent ionization NO^+ and doubly ionized NO^{2+} (multiplied by a factor of 10). Experimental data are from Kim *et al.*,[66] Iga *et al.*,[30] Lindsay *et al.*,[29] and Lopez *et al.*[31] Double ionization constitutes about 2% of the total ionization cross section in NO.

3. N_2O

N_2O is a closed shell, linear molecule with an N–N–O geometry.

3.1. Total scattering cross section

Early measurements of the TCS by Ramsauer[71] extended from 0.15 eV to 1.25 eV and were performed with an apparatus with a perpendicular magnetic field and the radius of electron trajectories of

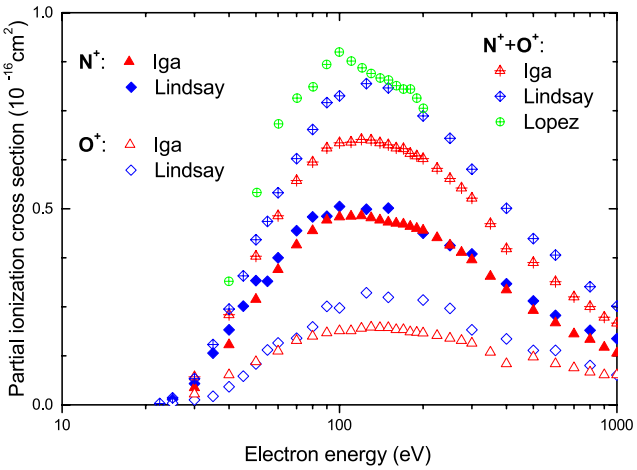

FIG. 16. Partial ionization cross sections for ionization of NO by electron impact: fragment N^+ and O^+ ions and the summed ($N^+ + O^+ + NO^{2+}$ ion signal unresolved in measurements of Lopez *et al.*). Experimental data are from Iga *et al.*,[30] Lindsay *et al.*,[29] and Lopez *et al.*[31]

Published by AIP Publishing on behalf of the National Institute of Standards and Technology.

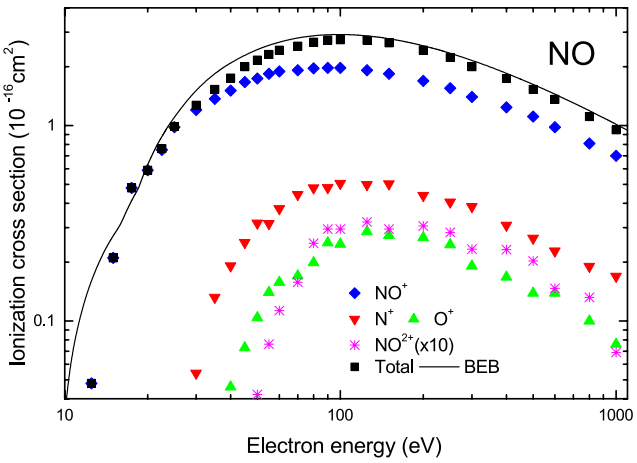

FIG. 17. Recommended total and partial cross sections for electron-impact ionization of nitric oxide, NO. Data are based on the experiment by Lindsay *et al.*[29] apart from NO^{2+} cross sections which up to 180 eV are based on data from Innsbruck.[66] The BEB model for total ionization by Hwang *et al.*[32] The uncertainties are ±5% on total ionization and NO^+, ±15% on N^+, ±20% on O^+, and ±30% on NO^{2+} partial ionization cross sections.[27]

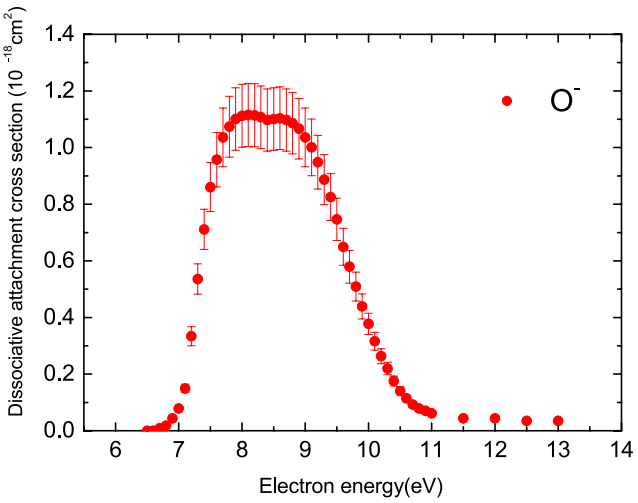

FIG. 18. Recommended dissociative attachment cross sections for the formation of O^- from NO.

8 mm. Those are only measurements extending below 1 eV and showing a rise of TCS toward zero energy, as it would be predicted from the polar character of the N_2O molecule.

Kwan *et al.*[33] measured TCS for electron and positron scattering between 1.25 and 500 eV using a long (109 cm), curved scattering cell with a guiding magnetic field and a retarding field analyzer. Szmytkowski and collaborators measured N_2O cross sections in several papers.[72–74] The main features of their apparatus were the same: a 127° cylindrical electrostatic selector and a rather short (30 mm) scattering cell, resulting in a modest (10^{-3} sr) geometrical angular resolution.

TABLE 8. Recommended dissociative attachment cross sections (CS's) for the formation of O^- from NO in 10^{-18} cm^2. Energy in eV

Energy	CS	Energy	CS	Energy	CS
6.7	0.0088	8.3	1.109	9.9	0.440
6.8	0.0176	8.4	1.100	10.0	0.378
6.9	0.0440	8.5	1.103	10.1	0.317
7.0	0.0792	8.6	1.106	10.2	0.264
7.1	0.150	8.7	1.100	10.3	0.220
7.2	0.334	8.8	1.088	10.4	0.176
7.3	0.537	8.9	1.069	10.5	0.141
7.4	0.713	9.0	1.040	10.6	0.114
7.5	0.862	9.1	1.000	10.7	0.0924
7.6	0.959	9.2	0.950	10.8	0.0792
7.7	1.040	9.3	0.888	10.9	0.0704
7.8	1.076	9.4	0.827	11.0	0.0616
7.9	1.103	9.5	0.748	11.5	0.0440
8.0	1.115	9.6	0.651	12.0	0.0440
8.1	1.117	9.7	0.581	12.5	0.0352
8.2	1.116	9.8	0.510	13.0	0.0352

The first series of measurements[72,74] were made without a retarding field analyzer, so were possibly subject to an underestimation due to the nondiscrimination of inelastically scattered projectiles. In fact, remeasured values[21] at energies above 10 eV (i.e., above thresholds for electronic excitation) are higher than earlier data and agree with those by Kwan *et al.* (Fig. 19).[33]

In the region of the low-energy $^2\Pi$ resonance,[75,76] the agreement between Szmytkowski *et al.*[72] and Kwan *et al.*[33] is pretty good, considering that small errors in the determination of the energy scale may significantly change the TCS measured. A high (approximately 1/3 of the TCS[77]) contribution comes in this resonance from the vibrational cross section. As noted subsequently by Johnstone and Newell,[78] the temperature of the gas, via vibrational excitation, can also influence this resonance maximum.

Xing *et al.*[35] used a 202 mm long collision chamber and a 70 mm long drift distance between the chamber and the analyzer equipped with a retarding field, obtaining an angular resolution of 6.3×10^{-5} sr. Their data[35] match very well with those by Kwan *et al.*[33] This matching is also confirmed by the B-B plot (see Fig. 2). The parameters of this plot [see Eq. (1)] are $A = -75 \pm 10$ and $B = 467 \pm 5$. The level of confidence on the B-B fit in N_2O is higher than in NO, thanks to high-quality of data by Xing *et al.*[35] extending up to 4250 eV.

Generally, after the above-mentioned considerations, agreement between different sets of data[34,35,71,72] is good, within ±10% in the whole energy range from tenths of electron volts to 1 keV. The recommended TCS are based on Ramsauer's measurements[71] at lowest energies, matching with those by Kwan *et al.*[33] in the region of the $^2\Pi$ resonance, on the mean values between Kwan *et al.* and Szmytkowski *et al.*[21] above 10 eV, and on Xing *et al.*'s TCS in the high energy limit. The recommended values are given in Table 9; they coincide with those from Ref. 13.

3.2. Elastic scattering cross section

There have been many reports on the experimental measurements of elastic DCS and ICS for N_2O molecule. Among them, the

Published by AIP Publishing on behalf of the National Institute of Standards and Technology.

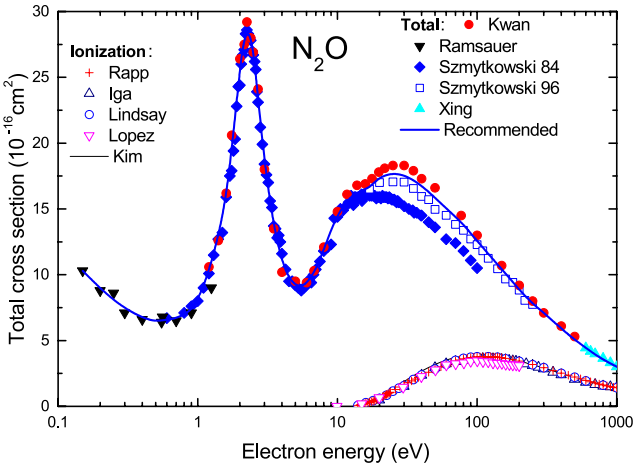

FIG. 19. TCS's for electron scattering on nitrous oxide, N_2O. Experimental absolute TCS's are from Ref. 33—full circles (digitalized from their figure), from Ref. 71—inverted triangles, Refs. 72 and 74—full diamonds, Ref. 21—open squares, and Ref. 35—full triangles. The thick line represents our recommended TCS. Ionization ICS—experiments: Rapp and Englander-Golden,[28] Iga *et al.*,[30] Lindsay *et al.*,[27] and Lopez *et al.*;[31] BEB model by Kim *et al.*[67]

most relevant results to this evaluation are the following. Marinkovic *et al.*[73] reported the absolute DCS's and ICS's for the energy range from 10 eV to 80 eV and for the angular range of 8°–150°. Later, Johnstone and Newell[78] measured the DCS's and ICS's for 5 eV–80 eV energy and 10°–120° angles. Kitajima *et al.*[79] performed an experiment to measure DCS's for 1.5–100 eV energy and 20°–130° angular range. Their work was supplemented by the work of the Australian National University (ANU) group in the report of Kitajima *et al.*,[80] which presented the cross sections of both Sophia University group and the ANU group. The ANU group measured the cross sections for the energy range of 2.0–20 eV and the angular range of 20°–130°. Finally, Lee *et al.*[81] reported the absolute DCS's and ICS's for 50–800 eV and 15°–130° ranges. Excluding the work of Marinkovic *et al.*,[73] which shows deviations from the other results especially at high angles, we estimate the recommended DCS's and ICS's values and their corresponding uncertainties for the electron impact energies at 1.5, 3.0, 5.0, 10, 15, 20, 30, 50, 100, and 500 eV. Numerical values of these cross sections and four representative figures for elastic DCS's are presented in Table 10 and Fig. 20, respectively. Similarly, the recommended ICS's are given in Table 11 and Fig. 21.

3.3. Momentum transfer cross section

Pack *et al.*[82] measured the drift velocity of slow electrons in pure N_2O at two different gas temperatures, 195 K and 300 K, and derived a momentum transfer cross section as a function of electron energy over the energy range between about 0.008 and 0.05 eV. It should also be added that they observed no appreciable dependence of the drift velocity on the gas temperature, and therefore, the contribution of rotational excitation and de-excitation processes to electron swarms cannot be substantial in pure N_2O. Singh[83] calculated the momentum transfer cross section using effective-range theory[84] in the energy range 0.01–0.1 eV. These two studies covered almost overlapping energy range and resulted in a very good agreement between them.

TABLE 9. Recommended TCS (in 10^{-16} cm^2) for electron scattering on nitrous oxide N_2O. Recommended values up to 10 eV are based on experimental data,[33,71,72] at 10–250 eV—on experimental data,[21,33] and on Ref. 35 above 500 eV. The uncertainty in the recommended data is ±10%

Electron energy	TCS	Electron energy	TCS	Electron energy	TCS
0.15	10.3	2.7	23.5	60	15.0
0.20	9.0	3.0	18.6	70	14.4
0.25	8.1	3.5	13.6	80	13.8
0.30	7.5	4.0	11.0	90	13.2
0.35	7.1	4.5	9.73	100	12.6
0.40	6.8	5.0	9.24	120	11.6
0.45	6.6	5.5	9.17	150	10.4
0.50	6.5	6.0	9.37	170	9.78
0.60	6.6	7.0	10.4	200	8.87
0.70	6.7	8.0	11.9	250	7.80
0.80	7.0	9.0	13.4	300	7.12
0.90	7.4	10	14.5	350	6.46
1.00	8.1	12	15.9	400	5.92
1.20	10.2	15	16.4	450	5.47
1.50	14.3	17	16.6	500	5.08
1.70	18.1	20	17.4	600	4.44
2.00	25.6	25	17.7	700	3.94
2.10	27.3	30	17.6	800	3.56
2.20	28.2	35	17.2	900	3.26
2.30	28.4	40	16.7	1000	3.01
2.40	27.9	45	16.3		
2.50	26.9	50	15.8		

Published by AIP Publishing on behalf of the National Institute of Standards and Technology.

TABLE 10. Recommended elastic DCS for N_2O. DCS's and uncertainties (δ) are in units of 10^{-16} cm^2 sr^{-1}

	1.5 (eV)		3.0 (eV)		5.0 (eV)		10.0 (eV)		15.0 (eV)		20.0 (eV)		30.0 (eV)		50.0 (eV)		100.0 (eV)		500.0 (eV)	
Angle (deg)	DCS	δ	DCS	δ	DCS	δ	DCS	δ	DCS	δ	DCS	δ	DCS	δ	DCS	δ	DCS	δ	DCS	δ
10							4.43	0.53	8.26	0.99	33.8	4.05	29.9	3.6	23.2	2.78				
15							3.95	0.6	6.44	1.01	8.55	1.32	12.9	1.55	12.6	3.74	7.66	1.53	1.237	0.148
20	1.50	0.23	1.63	0.24	0.61	0.11	2.92	0.46	4.88	0.71	5.61	1	5.76	1.14	5.67	1.68	3.32	0.84	0.803	0.096
25					0.65	0.05	2.41	0.39	4.12	0.49					3.41	0.68	1.62	0.32	0.603	0.072
30	0.96	0.14	1.78	0.27	0.69	0.13	2.05	0.32	2.96	0.43	3.04	0.58	2.55	0.5	1.97	0.47	0.95	0.24	0.459	0.055
35			1.75	0.12	0.85	0.06	1.74	0.25	2.68	0.32					1.26	0.25	0.55	0.11	0.3	0.036
40	0.67	0.10	1.72	0.28	0.87	0.17	1.48	0.23	1.9	0.26	1.73	0.28	1.24	0.24	0.82	0.19	0.34	0.09	0.171	0.021
45			1.71	0.12	1.01	0.07	1.32	0.19	1.72	0.21					0.5	0.1	0.22	0.04	0.107	0.013
50	0.46	0.07	1.67	0.28	0.99	0.16	1.21	0.2	1.35	0.18	1.16	0.19	0.74	0.14	0.41	0.11	0.18	0.04	0.084	0.01
55			1.54	0.11	1.03	0.08	1.11	0.16	1.27	0.15					0.25	0.05	0.15	0.03	0.071	0.009
60	0.32	0.05	1.47	0.24	1.04	0.17	1.02	0.16	1.03	0.14	0.8	0.13	0.45	0.09	0.21	0.06	0.13	0.04	0.058	0.007
65			1.32	0.09	1	0.07	0.92	0.15	0.96	0.12					0.13	0.03	0.11	0.02	0.046	0.006
70	0.30	0.05	1.14	0.19	0.94	0.16	0.83	0.15	0.8	0.11	0.57	0.09	0.27	0.07	0.14	0.03	0.1	0.03	0.035	0.004
75			1.04	0.07	0.89	0.07	0.78	0.12	0.74	0.09	0.47	0.06	0.17	0.02	0.16	0.04	0.08	0.02	0.028	0.003
80	0.30	0.05	0.86	0.15	0.82	0.13	0.69	0.11	0.61	0.09	0.37	0.06	0.16	0.03	0.12	0.03	0.08	0.02	0.024	0.003
85			0.79	0.06	0.75	0.06	0.62	0.09	0.54	0.06	0.28	0.03	0.17	0.02	0.11	0.03	0.07	0.01	0.022	0.003
90	0.35	0.05	0.65	0.11	0.68	0.11	0.53	0.08	0.41	0.06	0.26	0.04	0.17	0.03	0.1	0.02	0.08	0.02	0.018	0.002
95			0.59	0.04	0.6	0.04	0.47	0.08	0.35	0.05	0.26	0.03	0.21	0.03	0.1	0.03	0.08	0.02	0.016	0.002
100	0.46	0.07	0.45	0.08	0.51	0.09	0.43	0.07	0.31	0.05			0.24	0.04	0.1	0.02	0.09	0.02	0.015	0.002
105			0.41	0.03	0.45	0.03	0.4	0.06	0.31	0.07	0.31	0.04	0.27	0.03	0.13	0.03	0.09	0.02	0.014	0.002
110	0.56	0.08	0.34	0.06	0.39	0.07	0.41	0.08	0.37	0.06	0.35	0.05	0.29	0.06	0.16	0.04	0.11	0.03	0.015	0.002
115			0.31	0.02	0.32	0.03	0.45	0.08	0.5	0.06					0.22	0.04	0.12	0.02	0.014	0.002
120	0.66	0.10	0.28	0.05	0.3	0.06	0.53	0.09	0.53	0.09	0.49	0.07	0.34	0.06	0.28	0.07	0.13	0.04	0.014	0.002
125			0.28	0.02	0.26	0.02	0.63	0.15							0.37	0.07	0.15	0.03	0.014	0.002
130	0.76	0.11	0.31	0.05	0.26	0.05	0.76	0.18	0.7	0.13	0.7	0.13	0.43	0.06	0.46	0.09	0.16	0.05	0.014	0.002

Marinkovic *et al.*[73] reported the momentum transfer cross section as well as the integral elastic cross section between 10 eV and 80 eV. Johnstone and Newell[78] also determined the integral elastic and momentum transfer cross sections between 5 eV and 80 eV with the claimed errors of 20% and 25%, respectively. Recently, Lee *et al.*[81] reported a joint theoretical (combination of the Schwinger variational iterative method and the distorted-wave approximation)-experimental (crossed electron beam-molecular-beam geometry) study on electron-N_2O collisions over the energy range from 50 eV to 800 eV, which gave good agreement between theory and the measurements. Experimental uncertainty estimated in the absolute DCS over the range of the scattering angles between 15° and 130° was 12% in the 100–800 eV energy range and 20% elsewhere. After accounting for the extrapolation procedure, the overall uncertainties in the integral elastic and momentum transfer cross sections were estimated to be 16% in the 100–800 eV range and 24% elsewhere. Again agreement between theory and measurement for the ICS's was good. Since the above four studies reported the elastic DCS's that are mutually consistent well within their claimed uncertainty limits, the elastic momentum transfer cross sections derived from their differential elastic cross sections should also be reliable.

Hayashi[85] determined a set of electron collision cross sections including the momentum transfer cross section for N_2O from electron swarm parameters (drift velocity, lateral diffusion coefficient, and ionization and attachment coefficients measured in pure N_2O) available at the time of compilation for electron energies up to 1000 eV. Electron swarm parameters in pure molecular gas in low and intermediate E/N depend on both the elastic momentum and vibrational excitation cross sections, and therefore, it is not possible, in principle, for the electron swarm study to determine both momentum and vibrational cross sections uniquely if it uses only swarm parameters measured in pure molecular gas. This is the long-standing uniqueness problem of current swarm studies. Nakamura[86] determined a cross section set for the molecule after his measurements of drift velocity and longitudinal diffusion coefficient in pure N_2O and also in dilute N_2O–Ar mixture. The sharp Ramsauer minimum in the elastic momentum cross section of the Ar atoms, which are the major constituent of the mixture, seems to "amplify"[87] the effect of vibrational energy loss of electrons in N_2O–Ar mixtures and gives rise to prominent E/N dependence in electron swarm parameters, which provides a very good guide for unfolding vibrational excitation cross sections. This fact suggests simultaneous use of swarm data measured in pure molecular gas and its dilute Ar (or any of other rare gases with the Ramsauer-Townsend minimum) mixtures can help the swarm study to determine the elastic momentum transfer cross section and the vibrational excitation cross sections almost separately. The momentum transfer cross sections from the two swarm methods agree well in the energy range up to 0.1 eV, where the two agree with those of Pack *et al.*[82] and Singh,[83] and also in the range above 5 eV, where the two agree with the data from crossed

Published by AIP Publishing on behalf of the National Institute of Standards and Technology.

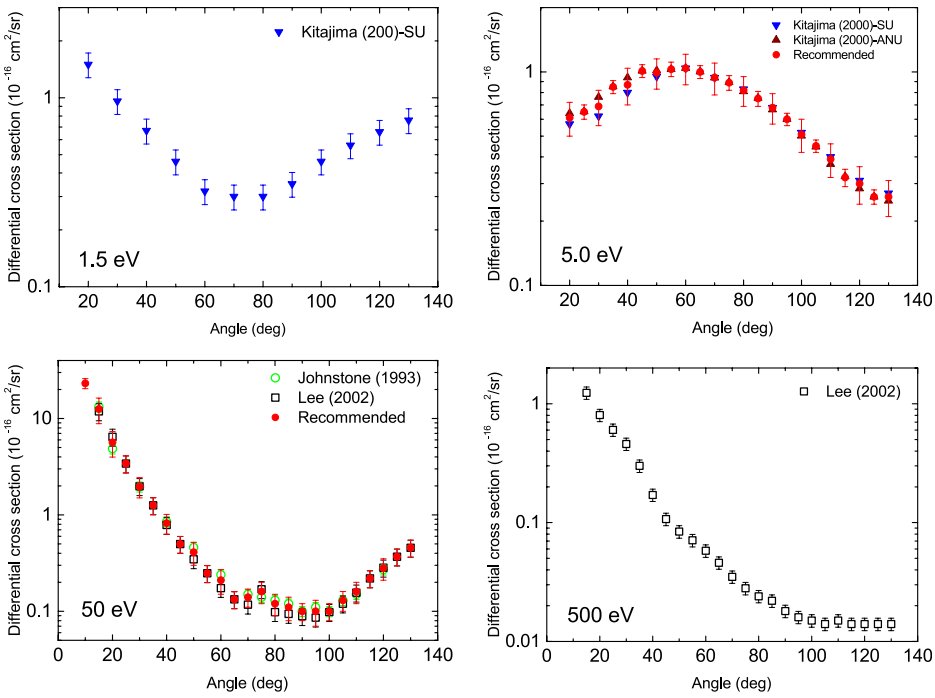

FIG. 20. Recommended elastic DCS for four representative energies.

beam experiments.[73,78,85] They all can be chosen as the recommended cross section in the respective energy ranges. For the remaining energy range, 0.1–5 eV, which almost exactly corresponds to the range of vibrational cross sections, the momentum cross section of Nakamura is recommended. As explained above, this recommended[86] cross section, together with his vibrational cross sections, can reproduce swarm parameters in pure N_2O and N_2O–Ar mixture simultaneously (see Sec. 3.5). Available momentum transfer cross sections are compared in Fig. 22. The present recommended cross section data that consist of Nakamura (up to 100 eV) and Hayashi (100–1000 eV) are also shown in Table 12.

3.4. Rotational excitation cross sections

There are no data on rotational excitation of the N_2O molecule in the literature. As part of this study, we computed excitation cross sections using the UK R-matrix[88,89] and the POLYDCS[90] codes. It is worth mentioning that *ab initio* calculations of the N_2O equilibrium geometry and the electric dipole were also performed in this study. At the equilibrium geometry, the N–N and N–O distances were found to be 1.122 Å and 1.173 Å, which is similar to the experimental and previous theoretical values.[91] The theoretical value of the dipole moment is about 0.38 ± 0.04 D, with the uncertainty mainly due to the

TABLE 11. Recommended elastic ICS and uncertainties (δ) for N_2O in units of 10^{-16} cm^2. Energy in eV

Electron	ICS	δ	Energy	ICS	δ
2	11.4	4.3	30	12.3	2.0
3	10.7	3.9	50	10.1	3.2
4	7.9	2.8	80	8.0	1.9
5	8.4	2.0	100	6.6	1.1
6	7.9	2.8	150	5.7	0.9
7	8.3	2.1	200	4.1	0.7
8	10.1	3.0	300	3.8	0.6
9	11.1	2.8	400	3.1	0.5
10	12.8	3.9	500	2.3	0.4
15	15.3	5.3	800	1.9	0.3
20	14.3	4.3			

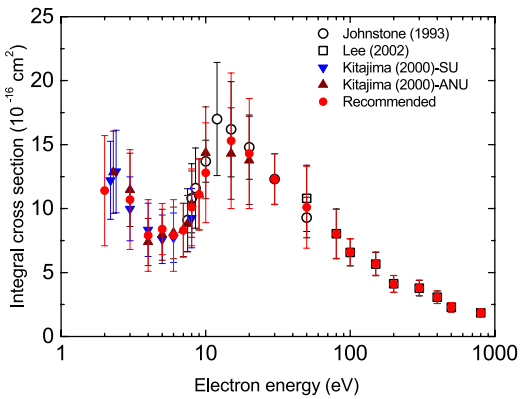

FIG. 21. Recommended elastic ICS for N_2O.

Published by AIP Publishing on behalf of the National Institute of Standards and Technology.

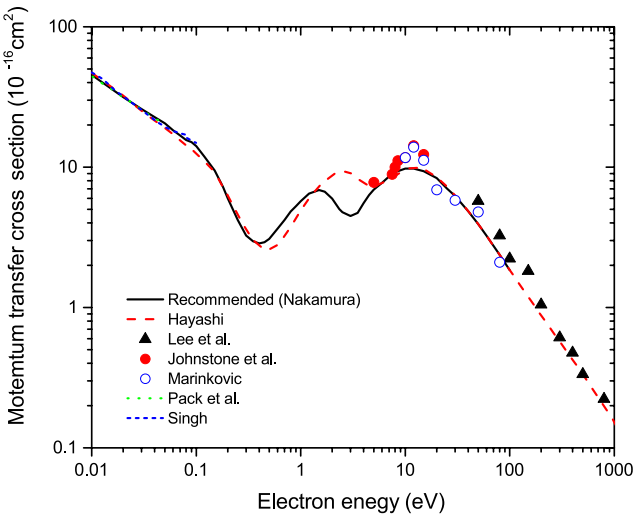

FIG. 22. Momentum transfer cross section. Dotted line, Pack, Voshall, and Phelps;[82] short broken line, Singh;[83] open circle, Marinkovic *et al.*;[73] solid circle, Johnstone and Newell;[78] solid triangle, Lee *et al.*;[81] broken line, Hayashi,[85] and solid line, Nakamura.[86]

uncertainty in the equilibrium geometry. This value is much larger than the experimental value of 0.161 D but is consistent with previous theoretical results.[91] The reason for the disagreement could be the following: For an accurate comparison with the experimental value, the theoretical dipole moment should be averaged over the wave function of the ground vibrational level of N_2O. The difference between the experimental dipole and theoretical value obtained at the equilibrium geometry could be explained by a combined effect of a relatively strong linear dependence of the theoretical dipole as a function of internuclear distances and nonharmonicity of the N_2O potential near the equilibrium. For completeness, it should also be mentioned that another experimental study[92] gave a value for the dipole of 0.52 ± 0.45 D, which is closer to the theoretical result, but due to a large uncertainty, it is also consistent with the experimental value of 0.161 D by Reinartz *et al.*[93] For the calculation, theoretical dipole moment of 0.38 D and the equilibrium geometry were employed. The cross sections obtained are shown in Fig. 23.

3.5. Vibrational excitation cross sections

The molecule N_2O has three fundamental vibrational modes: ν_1 (NN stretch, 0.276 eV), ν_2 (bend, 0.073 eV), and ν_3 (NO stretch, 0.159 eV).[94] Hayashi[85] proposed cross sections for electron collision excitation to those three vibrational states from electron swarm parameters in pure N_2O. Kitajima *et al.*[80] measured DCS's for vibrational excitations of three fundamental modes at 2.4 eV and 8.0 eV. Uncertainties for these DCS's were estimated between 30% and 50%. ICS's were also determined. Allan and Skalicky[95] also measured absolute DCS's for the elastic and the vibrationally inelastic electron scattering including three fundamental modes and several other overtones. The scattering angle was fixed at 135°, but the measurements covered electron energy range from the threshold region up to 20 eV including $^2\Pi$ resonance at 2.4 eV and a resonance at 8 eV. Each of the measured DCS's is multiplied by a factor 4π and an ICS is estimated here. The results compare very well with those of Kitajima *et al.*, as shown in Fig. 24. Electron drift velocity in dilute N_2O–Ar mixture shows[86] a peculiar E/N dependence with two humps, which may suggest vibrational excitation cross sections with two distinct peaks at threshold and shape resonance energies. By utilizing the DCS's of Allan and Skalicky[95] and by following the procedure explained in Sec. 3.3, Nakamura derived cross sections for three

TABLE 12. Recommended momentum transfer cross section for N_2O in units of 10^{-16} cm^2. Energy in eV

Electron energy	MT	Electron energy	MT	Electron energy	MT
0	500	0.3	3.26	4.50	6.32
0.001	139	0.35	2.96	5.0	6.92
0.002	100	0.40	2.86	6.0	7.73
0.005	63.1	0.45	2.92	7.0	8.60
0.01	45.4	0.5	3.08	8.0	9.22
0.02	31.6	0.6	3.65	10	9.75
0.03	26.0	0.7	4.20	12	9.75
0.04	22.7	0.8	4.83	15	9.35
0.05	20.5	0.9	5.27	20	8.36
0.06	18.3	1.0	5.72	25	7.06
0.07	16.8	1.2	6.49	30	6.22
0.08	15.6	1.5	6.87	40	4.85
0.09	15.1	1.7	6.68	50	3.93
0.10	14.1	2.0	5.97	60	3.25
0.12	11.9	2.34	5.02	80	2.37
0.15	9.48	2.5	4.77	100	1.85
0.18	7.23	3.0	4.49	200	0.848
0.20	6.00	3.5	4.72	500	0.306
0.25	4.20	4.0	5.55	1000	0.130

Published by AIP Publishing on behalf of the National Institute of Standards and Technology.

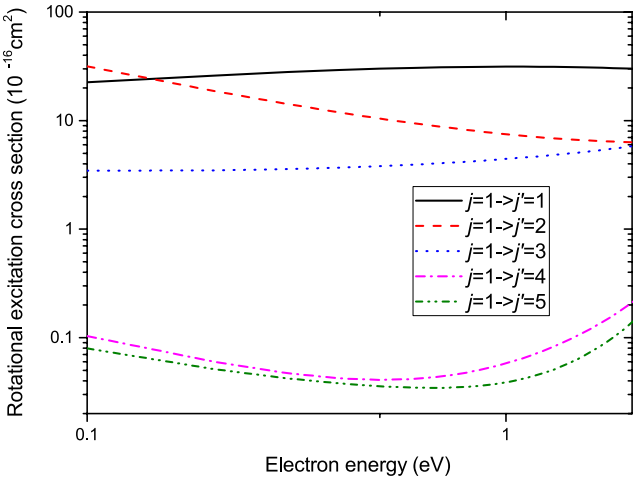

FIG. 23. Rotational excitation cross sections of the N_2O molecule computed using the UK R-matrix[88,89] and the POLYDCS[90] codes.

vibrational excitations: ν_2 (threshold: 0.073 eV), $\nu_3/2\nu_2$ (unresolved, threshold: 0.145 eV), and $\nu_1/2\nu_3$ (unresolved, threshold: 0.276 eV). The resultant cross sections of the first two vibrational excitations, ν_2 and $\nu_3/2\nu_2$, agree fairly well with those estimated from the work of Allan and Skalicky, and the magnitude of the $\nu_1/2\nu_3$ cross section at the shape resonance is about an order of magnitude larger than that of Allan and Skalicky. These larger cross sections, however, reproduce the experimental electron drift velocity measured in an N_2O–Ar mixture and also in pure N_2O when combined with the recommended momentum transfer cross section discussed above. As discussed below, the magnitude of the recommended vibrational excitation cross sections and the experimental elastic ICS of Kitajima *et al.*[80] can be added up to make the TCS that is consistent with the recommended total scattering cross section around the shape resonance region, which acts to support our recommended values.

3.6. Electronic excitation cross section

Investigations on the location and assignment of electronic excitation states for the N_2O molecule have been carried out through studies on optical absorption[96] and electron energy loss spectrum.[97,98] Cubric *et al.*[99] obtained the first high-resolution (30–40 meV resolution) electron impact spectrum of N_2O over the energy range from 1.5 to 21 eV and gave a detailed assignment of the observed structures, including the valence states as well as the Rydberg states. Electronic excitation in N_2O (into optically allowed states), as seen in zero-degree energy-loss spectra (see Fig. 25), is dominated by two broad peaks labeled C $^1\Pi$ and D $^1\Sigma^+$ states.

Michelin, Kroin, and Lee[100] reported differential and ICS's for electronic excitations to the C $^1\Pi$ state and the $^3\Pi$ state (8.0 eV energy loss) in the 10–100 eV range by using the distorted-wave method.

In the work of Kawahara *et al.*,[101] ICS's (see Figs. 26 and 27) were obtained using extrapolated DCS's to zero-angle scattering via GOS. As admitted by them, the use of GOS is not fully appropriate at low scattering energies. Therefore, they also applied a semiempirical

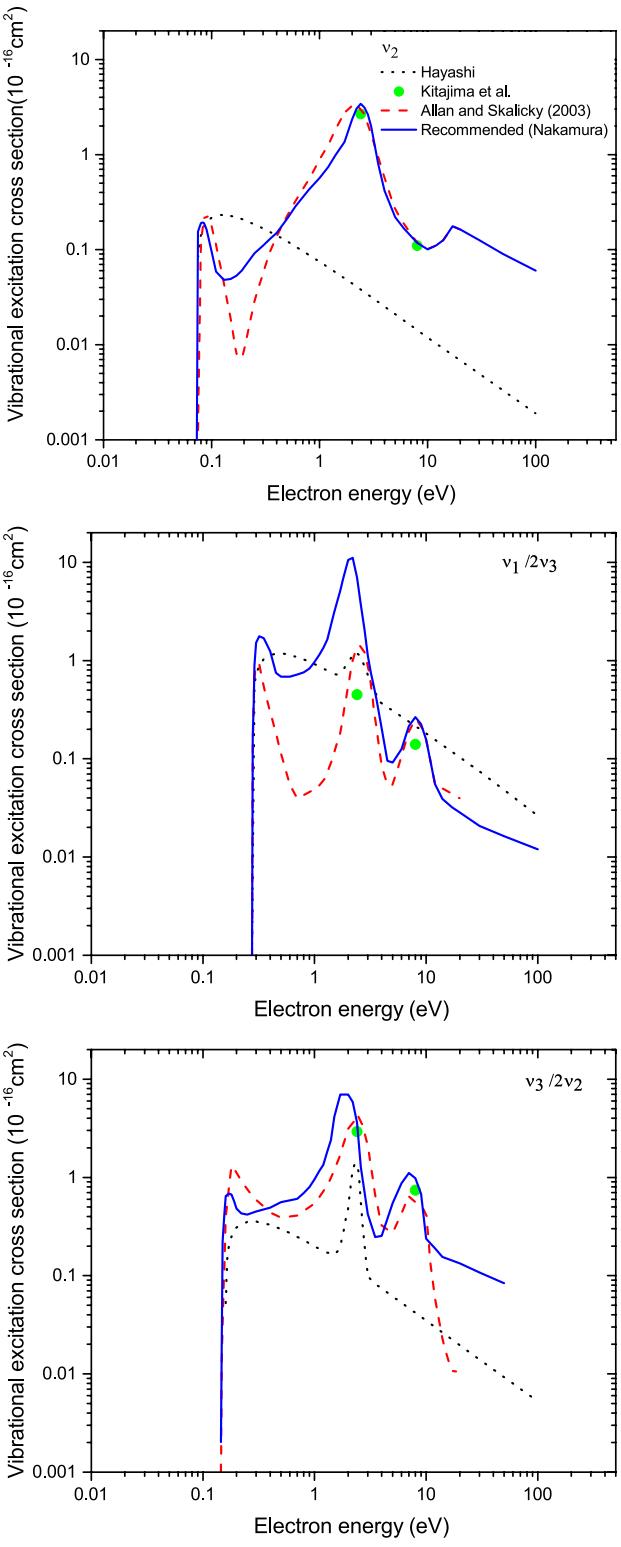

FIG. 24. Vibrational excitation cross sections. Solid circle, Kitajima *et al.*;[80] dotted curve, Hayashi;[85] broken curve, Allan and Skalicky;[95] and solid curve, Nakamura.[86]

Published by AIP Publishing on behalf of the National Institute of Standards and Technology.

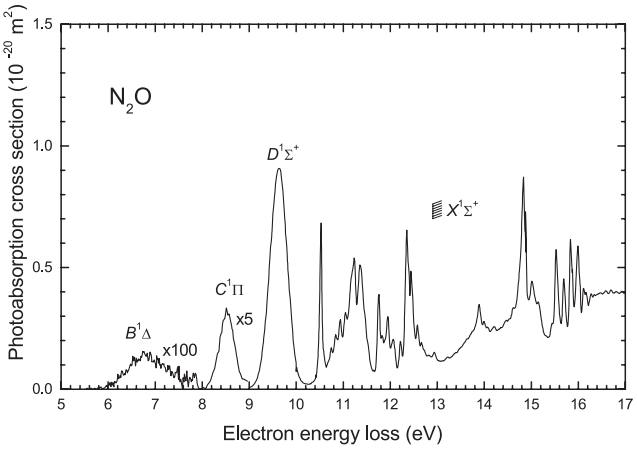

FIG. 25. Zero-angle electron-scattering energy loss spectra in N_2O from experiments by Chang *et al.*[51] The ionization threshold is 12.89 eV for N_2O.

approach of Kim,[57] based on the scaling of the Born approximation to effective scattering energy (BE approach) and with the use of GOS (*f*-factors) from experiment (so-called BE*f* scaling).The results of Kawahara *et al.* for the C $^1\Pi$ and D $^1\Sigma^+$ states are shown in Figs. 26 and 27. BE*f* results agree with the experiment starting from the collision energy of 50 eV.

Marinković *et al.*[73] measured DCS for C $^1\Pi$ and D $^1\Sigma^+$ states at 0°–148° scattering angles and 15–80 eV collision energy. Only for 80 eV do they give absolute values of the DCS via normalization to their own[73] elastics DCS (that, in turn, were normalized to TCS). Errors on DCS were estimated as 32%. In 1999, Marinković *et al.*[102] renormalized the DCS using the GOS evaluated from comparison

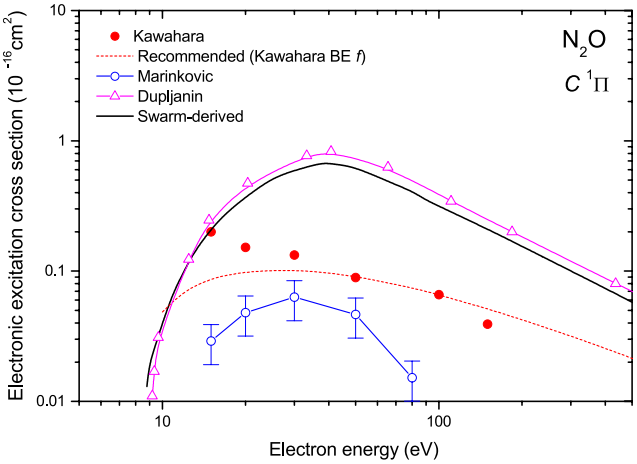

FIG. 26. ICS's for the excitation of N_2O into the C $^1\Pi$ state. Absolute measurements by Kawahara *et al.*[101]—full circles; normalized (see text) measurements by Marinković *et al.*,[73,102] open circles. Two excitation cross sections used for swarm modeling: Dupljanin *et al.*[106] and present values ("swarm-derived")—lines with triangles and heavy chain lines, respectively. Broken lines, BE*f* model by Kawahara *et al.*[101]

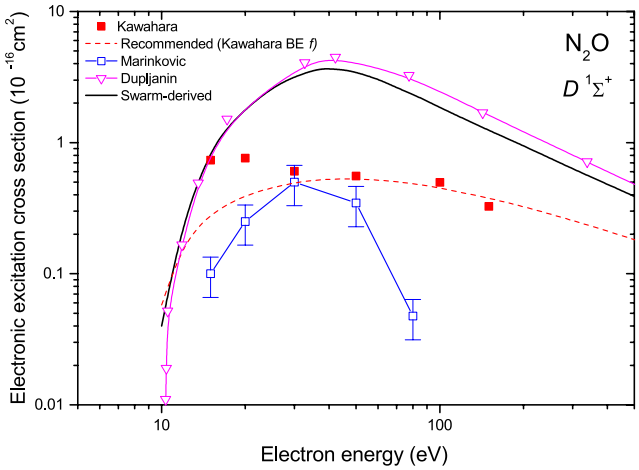

FIG. 27. ICS's for the excitation of N_2O into the D $^1\Sigma^+$ state. Absolute measurements by Kawahara *et al.*[101]—full squares; normalized (see text) measurements by Marinković *et al.*,[73,102] open squares. Two excitation cross sections used for swarm modeling: Dupljanin *et al.*[106] and present values ("swarm-derived")—lines with triangles and heavy chain lines, respectively. Broken lines, BE *f* model by Kawahara *et al.*[101]

between experiments and theory: in the limit zero-scattering angle, they adopted the optical oscillator strength of 0.026 and 0.375 for the C $^1\Pi$ and D $^1\Sigma^+$ states, respectively.

Figures 26 and 27 show ICS's for these two states obtained by multiplying the integral values given by Marinković *et al.*[73] by the coefficients given for DCS in Ref. 102. This is only a rough comparison: in particular, at high energies, these ICS's can be underestimated due to possible errors in forward-angle analysis of DCS's. In fact, the ICS of Marinković *et al.* for the D $^1\Sigma^+$ state at 30 eV coincides with that of Kawahara *et al.*,[101] but at higher energies, it falls much more rapidly with the energy (see Fig. 27).

We are not aware of experimental determinations of excitations into triplet states in N_2O. A recent theoretical evaluation[103] using the Quantemol-N R-matrix package[89] gives a narrow peak with a maximum of 0.25 $\times 10^{-16}$ cm^2 at 10 eV for the $^3\Sigma^+$ ($^3A_1$) state and similarly a narrow peak of 0.15 $\times 10^{-16}$ cm^2 at 14 eV for the $^3\Pi$ ($^3B_1$) state.

There is another assessment of the (total) cross section for electronic excitations by using an electron swarm method. Most electronic excitation thresholds of atoms and molecules lie immediately below the ionization threshold and the electron energy losses through electronic excitations can effectively determine the spread of the electron energy distribution that overlaps with the ionization cross section, namely, the threshold nature of the primary ionization coefficient. Experimental uncertainties of the ionization cross section and the primary ionization coefficient are usually low and are both about a few percent. A Boltzmann calculation shows small amendment to the threshold part of an electronic excitation cross section can alter the resultant primary ionization coefficient sensitively but only minimal change, if any, of any other swarm parameters like an electron drift velocity.

Swarm checks (see, for example, Refs. 104 and 105) show that underdetermination of the electronic excitation overestimates the transversal diffusion coefficient above 100 Td. The presently recommended set does not include cross sections for excitation into higher states, visible in the energy-loss spectra below the ionization

Published by AIP Publishing on behalf of the National Institute of Standards and Technology.

threshold (see Fig. 25). Therefore, the set of recommended cross sections to be used in modeling electron swarms has to "mimic" these missing contributions. For this reason, for swarm modeling, we recommend the set given in Table 13 and presented in Fig. 28, which also coincides with the set used by Duplijanin *et al.*[106] (see the comparison given in Figs. 26 and 27).

Thin solid curves in Fig. 28 show the three swarm-derived electronic excitation cross sections determined in order that they can reproduce the experimental primary ionization coefficient of pure N_2O[107] within a few percent. They are given realistic threshold energies but are by no means intended to be any specific excitation processes: they as a whole are only intended to provide realistic energy loss of electrons passing through the gas and, in fact, unique determination of their respective cross sections was not possible. However, it will be shown in the later section that the sum of these three swarm-derived cross sections, the recommended elastic cross section (Sec. 3.2), and the recommended ionization cross section (Sec. 3.8) agrees well with the recommended TCS (Sec. 3.1).

As recommended ICS's for excitation to the C $^1\Pi$ and D $^1\Sigma^+$ states, we adopt the BE*f* semiempirical values by Kawahara *et al.*[101] and for the B $^1\Delta$ state—the semiempirical BE values of Wang *et al.*[108] (see Table 13).

3.7. Dissociation cross section

The D $^1\Sigma^+$ excited state of N_2O is repulsive, leading to dissociation of the molecule. Several experiments revealed dissociation of N_2O into the oxygen atom in its ground state $O(^3P)$ and the N_2 molecule in electronically excited states (see Ref. 60 for the discussion). Le Clair and McConkey[60] studied the channel $e + N_2O \rightarrow e' + O(^1S) + N_2(X\ ^1\Sigma_g^+)$ with production of the metastable (i.e., second excited level) oxygen atom $O(^1S)$. Measurements were performed via detection of optical emission from the XeO* excimer. Normalization was performed adopting the optical oscillator strength of 0.36; the declared uncertainty on the cross section for the oxygen atoms $O(^1S_0)$ is 10%. The maximum of the cross sections is 0.225×10^{-16} cm^2 at 45 eV. We note that the cross section for production of the $O(^1S)$ atom is exactly half of the excitation to the D $^1\Sigma^+$ state, as obtained by Kawahara *et al.*[101] in their BE*f* model.

3.8. Ionization cross section

The agreement between different experiments[27,28,30,31] in N_2O is good, within 5% in the maximum of the total ionization cross section (see Fig. 29). In particular, the most recent experiment by Lindsay *et al.*[27] coincides with that by Rapp, Englander-Golden, and Briglia;[109] some differences exist in the low-energy part: data of Lopez[31] are higher than other sets, and measurements of Iga[30] are lower in the threshold region. More significant differences are to be noted for the parent N_2O^+ ion yield (see Fig. 30). Somewhat akin to the parent ion in the ionization of NO, the data of Iga *et al.*[30] and Lopez[31] for N_2O^+ are higher than those by Lindsay *et al.*[27] The experiment from Innsbruck,[65] using normalization to Ar^+, agrees with Lindsay *et al.* Note also that the shape of the optical emission curve[111] from the A $^2\Sigma^+$ excited state of N_2O coincides with the N_2O^+ yield by Lindsay *et al.*[27] (see Fig. 30). The difference in N_2O^+ formation seems to be "compensated" in partial cross sections for N^+ and O^+ formation, where data by Linsday *et al.*[27] are at the maximum higher by a factor of 2 than those by Iga *et al.*[30] and Lopez *et al.*[31] (see Fig. 31). A hint for resolving this discrepancy could come from early measurements by Märk *et al.*,[65] with a long, double E-M mass selector. In that experiment, the elapsed time between the instant of ionization and detection was longer than 14 μs. Märk *et al.* noted that normalization of their data to the Ar^+ signal of Rapp and Englander-Golden[109] gave the N_2O^+ cross section lower by some 40% than normalization to the dissociative ionization.[109] By changing ion optics, Märk *et al.* evaluated the metastable N_2O^{+*} to N_2O^+ ratio as 11%. Thus, using Märk *et al.*'s reasoning, the difference between the two groups of data for N_2O^+ production is due to the fragmentation of the metastable N_2O^{+*}

TABLE 13. Recommended cross sections for electronic excitation of N_2O into B $^1\Delta$, C $^1\Pi$, and D $^1\Sigma$ states, from the BE scaling model[101] in 10^{-18} cm^2 units. Uncertainty of this determination is ±20%. The last column is the sum of electronic excitations, as needed to reproduce swam coefficients (present work). The latter data are much higher than the sum of the three states: the swarm-derived cross sections account for the total energy loss due to electronic excitation, so they also comprise dipole-forbidden states; furthermore, they also account for the "effective" energy loss, i.e., for excitations into vibronic series

Energy (eV)	B $^1\Delta$	C $^1\Pi$	D $^1\Sigma$	Swarm-derived sum
5.65				10.7
5.70				17.8
5.8				25.4
6.0				29.7
6.3				36.7
6.6	0	0	0	41.1
7.0	0.712	0	0	44.8
7.4	1.48	0	0	46.7
7.8	1.92	0	0	
8.0				50.9
8.2	2.23	0	0	
8.6	2.47	0.636	0	
9.0	2.66	2.41	0	57.6
9.4	2.81	3.35	0	
10	2.98	4.35	4.79	74
11	3.19	5.57	11.2	
12	3.31	6.44	16.0	
15	3.41	8.00	27.1	185.7
20	3.27	8.98	38.5	
25	3.04	9.18	44.9	
30	2.82	9.08	48.5	331.7
40	2.43	8.58	51.3	
50	2.13	8.00	51.5	333.3
70	1.71	6.96	49 0.0	
100	1.32	5.8	44 0.0	210.1
150	0.965	4.54	37 0.0	
200	0.762	3.76	31.8	
300	0.54	2.82	25 0.0	
400	0.42	2.27	20.8	
500	0.344	1.92	17.9	45.2
600	0.292	1.66	15.7	
700	0.254	1.47	14.1	
800	0.225	1.32	12.8	
900	0.203	1.2	11.7	
1000	0.184	1.1	10.8	22.9

Published by AIP Publishing on behalf of the National Institute of Standards and Technology.

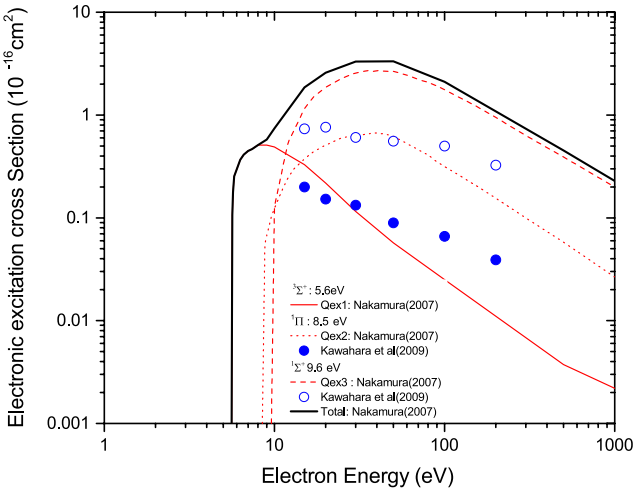

FIG. 28. Electronic excitation cross sections of N_2O. Closed and open circles, ICS[101] for excitations of C $^1\Pi$ and D $^1\Sigma^+$ states, respectively; three thin curves, swarm-derived excitation cross sections whose excitation threshold are assumed to be 5.6 eV (the value assigned to $^3\Sigma^+$), 8.5 eV (C $^1\Pi$), and 9.6 eV (D $^1\Sigma^+$), respectively; thick solid curve, sum of the swarm-derived cross sections.

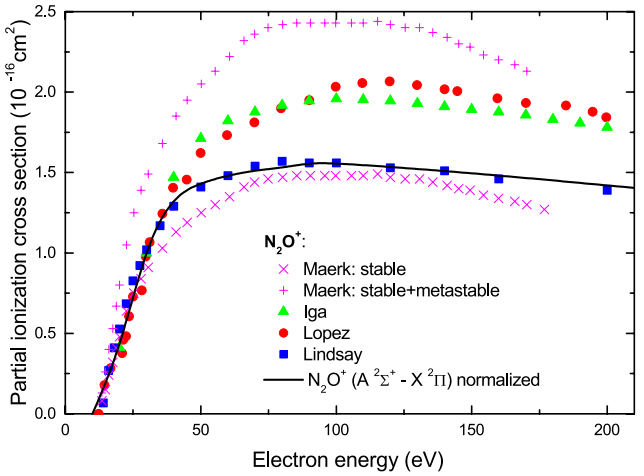

FIG. 30. Experimental[27,30,31,65] partial ionization for the parent ion N_2O^+. The optical emission for the A $^2\Sigma^+ \rightarrow X^2\Pi$ transition[111] (normalized by a factor of 4 to Lindsay *et al.*'s[27] N_2O^+ signal at 100 eV) is also shown.

ion. This, in turn, is not validated by the discussion of Lindsay *et al.*:[27] in their experiment, the time elapsed between the ionization and detection of N_2O^+ is 1.3 μs and the time between the electron pulse and extraction pulse is 200 ns. According to Newton and Sciamana,[112] the fragmentation time of N_2O^{+*} is only 90 ns. The NIST spectra[113] (4:1 ratio between N_2O^+ and NO^+ ions) at 70 eV would support the results of Iga *et al.*[30] and Lopez *et al.*[31] An updated evaluation of the N_2O^{+*} metastable yield is needed to resolve this issue. The recommended ionization cross sections for N_2O (see Fig. 32 and Table 14) are based on the data of Lindsay *et al.*[27] and coincide with those given by Lindsay and Mangan in their review:[27] this is a self-consistent set and summed partial cross sections agree with determinations of total ionization from other experiments.[30,31,109]

3.9. Electron attachment (DEA) cross section

Rapp and Briglia[69] measured the absolute TCS's for negative-ion formation in N_2O and some other gases by electron impact in a total ionization tube. Both dissociative attachment and ion-pair formation were measured, with careful attention paid to complete collection of the negative ions up to 50 eV electron energy. Their results showed a single peak at 2.2 eV, and the TCS for negative-ion formation at that

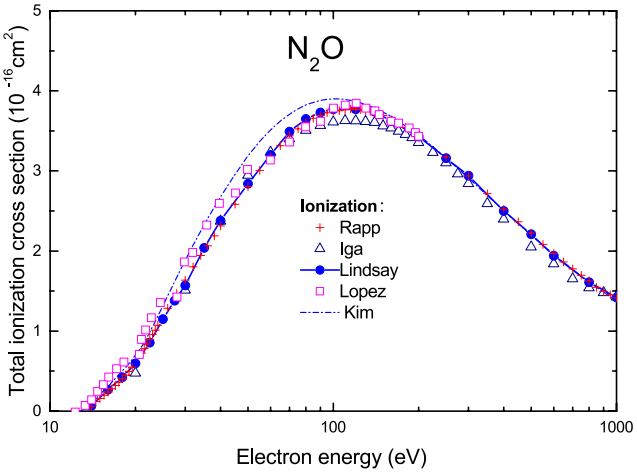

FIG. 29. Total ionization cross sections in N_2O: gross total—Rapp, Englander-Golden;[28] counting total—Iga *et al.*,[30] Lindsay *et al.*,[27] and Lopez *et al.*[31] Normalized data of Adamczyk *et al.*[110] coincide with Ref. 109. BEB model by Kim *et al.*[67] Recommended data are those by Lindsay *et al.*[27]

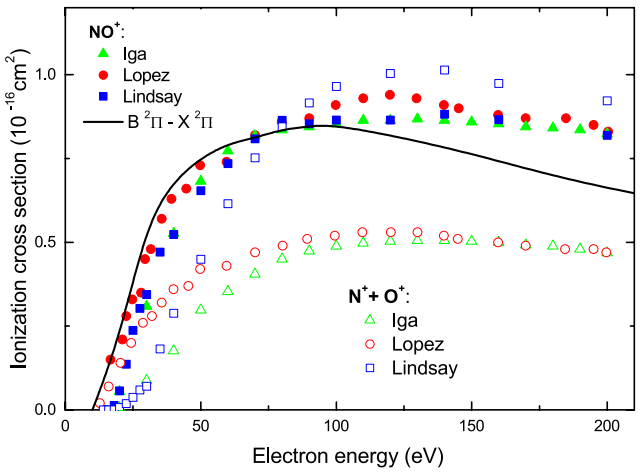

FIG. 31. Partial ionization of N_2O into NO^+ and (N^+ + O^+). Experimental data from Refs. 27, 30, and 31. The optical emission from NO^+ for the B $^2\Pi \rightarrow$ X $^2\Pi$ transition[111] (normalized by a factor of 40 to Lindsay *et al.*'s[27] NO^+ signal at 70 eV) is also shown.

Published by AIP Publishing on behalf of the National Institute of Standards and Technology.

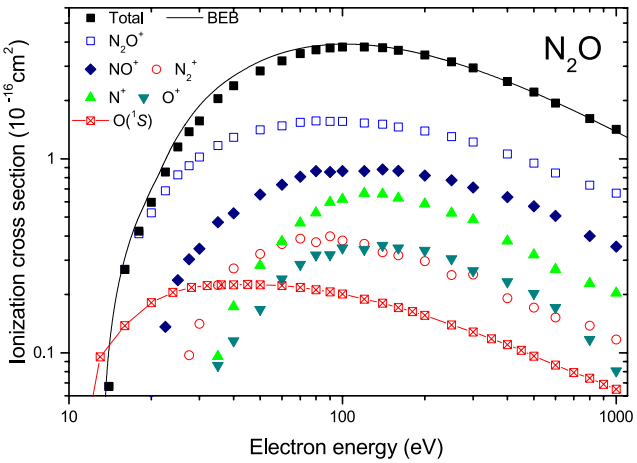

FIG. 32. Recommended cross sections for ionization of N_2O are based on Lindsay *et al.*[27] measurements and are the same as given by Lindsay and Mangan in their review.[27] The cross section for the formation of a neutral oxygen atom O in the $^1S_0$ electronic state measured by LeClair *et al.*[60] is also given: this comparison makes clear that the formation of the O atom is not a "coproduct" of ionization. BEB model by Kim *et al.*[67] The uncertainties are ±5% on total ionization and N_2O^+, ±10% on NO^+ and N^+, and ±15% on N_2^+ and O^+ partial ionization cross sections.[27]

energy was $9.78 \times 10^{-2}\pi\ a_0^2$. In this experiment, the negative-ion formed is believed to be mostly O^- from N_2O, inferred from the investigations of other studies such as the work of Krishnakumar *et al.*[114] Krishnakumar *et al.* measured the cross sections for the production of O^- from N_2O by the process of DEA for electron-impact energies ranging from 0 to 50 eV. Three new O^- peaks at 5.4, 8.1, and 13.2 eV were observed, and their data above 4 eV electron-impact energy differ from that of Rapp and Briglia.[69] The cross sections between about 1.5 and 4 eV agree well with Rapp and Briglia, but disagreements appeared again below about 1.5 eV. Krishnakumar[115] believes that one reason for their higher cross sections compared with Rapp and Briglia[69] below 1.6 eV may be due to heating of the gas by the magnetic coil they used inside the vacuum chamber. DEA in N_2O has a strong temperature dependence as was shown by Chantry.[116] Meanwhile, the problem with the data of Rapp and Briglia is that it is above 4 eV, where Krishnakumar *et al.*[114] observed three smaller clean peaks. Instead, Rapp found a broad peak at about 10 eV, and this might have been due to some impurities in the gas they used.[115] In addition, the Krishnakumar group has confirmed the peaks when they did the velocity map imaging experiments as shown in the work of Nandi *et al.*[117] Therefore, we recommend the cross sections of Rapp and Briglia[69] in the energy region between 1.6 eV and 4 eV. The uncertainty is given to be 15%. Our DEA cross sections are presented in Table 15 and Fig. 33, respectively. Above 4 eV, the results of Krishnakumar *et al.*[114] could be recommended, but they are very noisy, wiggly, and also blown up 40–70 times. So it is very difficult to extract precise numerical data by digitizing and no numerical values are available from the original authors.

4. NO_2

NO_2 is a free radical with one unpaired electron. Its X $^2A_1$ electronic ground state has a bent structure. There are less data available for NO_2 than NO or N_2O; this situation could be due to the difficulty with handling NO_2 molecules. NO_2 is corrosive and poisonous, and in the gas phase, it exists in equilibrium with N_2O_4 (dinitrogen tetroxide), which could cause a problem when performing experiments.

TABLE 14. Recommended cross sections for the ionization of N_2O are based on Lindsay *et al.*[27] measurements and are the same as given by Lindsay and Mangan in their review[27] in units of 10^{-16} cm^2. Energy in eV

Electron energy	CS N_2O^+	CS N_2^+	CS NO^+	CS N^+	CS O^+	CS total
14	0.067					0.067
16	0.269					0.269
18	0.411		0.0131			0.424
20	0.527	0.0066	0.0564		0.0066	0.597
22.5	0.684	0.017	0.136	0.0023	0.0163	0.855
25	0.827	0.047	0.237	0.0059	0.0315	1.15
27.5	0.922	0.097	0.303	0.0187	0.0407	1.38
30	1.02	0.141	0.344	0.0237	0.0466	1.57
35	1.17	0.223	0.471	0.0958	0.086	2.04
40	1.29	0.272	0.523	0.173	0.115	2.38
50	1.41	0.323	0.654	0.282	0.167	2.84
60	1.48	0.363	0.735	0.375	0.240	3.20
70	1.54	0.387	0.809	0.467	0.285	3.49
80	1.57	0.372	0.864	0.526	0.319	3.65
90	1.56	0.398	0.854	0.596	0.320	3.73
100	1.56	0.379	0.865	0.618	0.347	3.77
120	1.53	0.365	0.865	0.663	0.341	3.77
140	1.51	0.33	0.882	0.657	0.357	3.74
160	1.46	0.318	0.866	0.627	0.347	3.62
200	1.39	0.297	0.819	0.585	0.337	3.43
250	1.30	0.252	0.775	0.525	0.305	3.16
300	1.22	0.253	0.712	0.486	0.265	2.94
400	1.06	0.191	0.634	0.377	0.232	2.50
500	0.95	0.171	0.569	0.32 0	0.202	2.21
600	0.844	0.152	0.507	0.269	0.171	1.94
800	0.731	0.138	0.400	0.228	0.117	1.61
1000	0.666	0.117	0.353	0.203	0.0807	1.42

4.1. Total scattering cross section

Only few experiments have been performed on TCS in NO_2 due to the highly corrosive character of this gas. Szmytkowski and collaborators corrected[118] their earlier data[119] for the error due to collecting inelastically scattered electrons. The differences are similar to those in N_2O. However, corrected[118] data are higher than the measurements by Zecca *et al.*[36] in the high-energy limit. The reason for this discrepancy is unclear. Therefore, the recommended values at 100–350 eV are based on mean values from the three experiments;[21,36,119] at 7–100 eV on the newer measurements of Szmytkowski and Możejko,[21] and on the older ones[119] below 7 eV. The overall uncertainty on these data is to be estimated as ±15%. Theoretical calculations of TCS's were performed by Gupta *et al.*[120] who used the R-matrix method as implemented in the Quantemol-N package[89] below 15 eV and spherical complex optical potential. Above 50 eV, these calculations agree very well with the recommended data. Below 10 eV, the R-matrix method shows the presence of two narrow resonances, which were not visible in the experiments (see Fig. 34). Calculations show a

Published by AIP Publishing on behalf of the National Institute of Standards and Technology.

TABLE 15. Recommended dissociative attachment cross sections (CS's) for the formation of O^- from N_2O in units of 10^{-18} cm^2. Energy in eV

Energy	CS	Energy	CS
0.4	0.46	2.3	8.55
0.5	1.33	2.4	8.02
0.6	1.73	2.5	7.09
0.7	1.92	2.6	5.97
0.8	2.04	2.7	4.83
0.9	2.08	2.8	3.56
1.0	2.15	2.9	2.60
1.1	2.23	3.0	1.91
1.2	2.33	3.1	1.39
1.3	2.48	3.2	0.97
1.4	2.78	3.3	0.63
1.5	3.28	3.4	0.47
1.6	3.92	3.5	0.35
1.7	4.93	3.6	0.28
1.8	5.94	3.7	0.23
1.9	6.62	3.8	0.19
2.0	7.57	3.9	0.17
2.1	8.26	4.0	0.13
2.2	8.59		

steeper rise of the cross sections in the limit of zero energy than it is measured: a similar observation was made for another weakly polar molecule, NF_3 (see Ref. 3). For NO_2, the B-B plot is of poor quality, as the data by Zecca *et al.*[36] are underestimated above 1400 eV. A regression line would coincide with that for N_2O (Table 16).

4.2. Elastic scattering cross section

There are no experimental elastic DCS and/or ICS for NO_2 known to these authors at the time of evaluation. Therefore, we decided to recommend theoretical ICS's. There are several theoretical reports on elastic ICS's of NO_2. Mentioning a few relevant recent results, they are Joshipura *et al.*,[122] Munjal *et al.*,[123] and Gupta *et al.*[120] In Fig. 35, Joshipura *et al.*[122] and Gupta *et al.*[120] are presented. Also shown is the TCS of Szmytkowski *et al.*[119] to compare with the elastic ICS's. The two theoretical results diverge as the electron energies get smaller. Considering that the TCS measurements are generally more reliable than the other cross section measurements and that the uncertainty of the TCS of Szmytkowski *et al.*[119] in the range of 5–30 eV is 3%, the calculation of Gupta *et al.* seems to be overestimated, especially in this energy range. Therefore, we recommend Joshipura *et al.*[122] and the recommended ICS values are tabulated in Table 17.

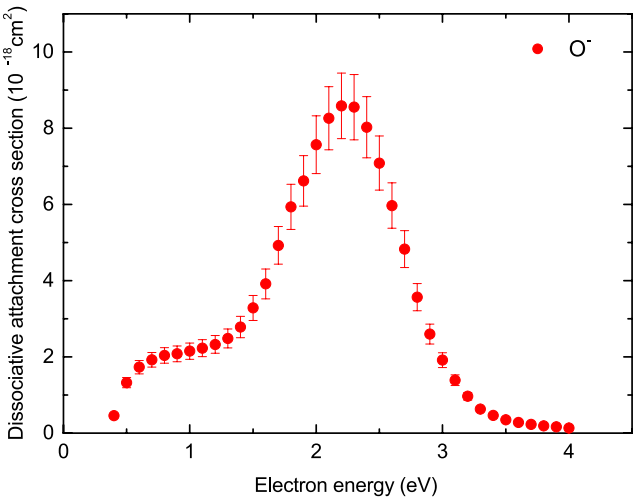

FIG. 33. Recommended cross sections for the formation of O^- from N_2O.

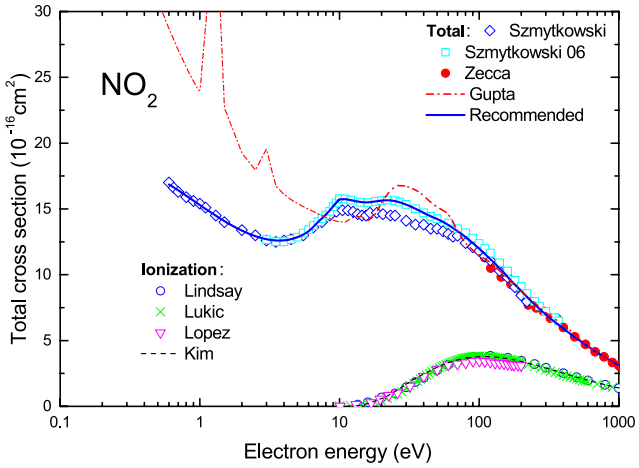

FIG. 34. TCS's for electron scattering on nitrogen dioxide, NO_2. Experimental absolute TCS's are from Szmytkowski *et al.*[119]—diamonds, from Szmytkowski and Możejko[34]—open squares, and from Ref. 36—full circles. Theoretical total:[120] Quantemol package below 15 eV and the optical model at higher energies. Thick line is the present recommended TCS. Ionization ICS—experiments: Lindsay *et al.*,[29] Lukić *et al.*,[121] and Lopez *et al.*;[31] BEB model by Kim *et al.*[67]

4.3. Momentum transfer cross section

Momentum transfer cross section for the NO_2 molecule were computed by Munjal *et al.*[123] using the R-matrix method[88] and POLYDCS.[90] The calculations of Munjal *et al.* are based on a 21-state close coupling expansion and suggest that the electron–NO_2 system supports a large number of resonances as might be expected, given the open shell nature of the target and the presence of several low-lying electronic states. The momentum transfer cross sections computed by Munjal *et al.* (see Fig. 36) show a significant structure due to these resonances. At present, these are the only momentum transfer cross section available for NO_2, but they must be considered somewhat uncertain.

4.4. Rotational excitation cross sections

There are no experimental data on rotational excitation of the NO_2 molecule, but the theoretical study by Munjal *et al.*[123] reported DCS's at one energy of 4 eV. That study used a somewhat large, compared to the experimental value, dipole moment of 0.738 D. Because the reported data are given only for one energy and the employed dipole moment was not accurate in Ref. 123, in this study,

Published by AIP Publishing on behalf of the National Institute of Standards and Technology.

TABLE 16. Recommended TCS (in 10^{-16} cm^2 units) for electron scattering on nitrogen dioxide NO_2. Recommended values up to 7 eV are based on experimental data by Szmytkowski *et al.*,[119] at 7–100 eV on the remeasurements by Szmytkowski and Możejko,[118] at 100–350 eV on the nonweighted average from the three experiments,[36,118,119] and on Ref. 36 above 350 eV. The uncertainty on the recommended data is ±15%

Electron energy	TCS	Electron energy	TCS	Electron energy	TCS
0.6	16.9	8	14.5	90	12.4
0.7	16.4	9	15.2	100	12.0
0.8	16.0	10	15.8	120	11.2
0.9	15.6	11	15.7	150	10.2
1.0	15.3	12	15.7	170	9.50
1.2	14.7	14	15.5	200	8.80
1.5	14.1	16	15.5	220	8.30
1.7	13.7	18	15.7	250	7.75
2.0	13.3	20	15.6	300	6.97
2.5	12.9	22	15.7	350	6.40
3.0	12.7	25	15.6	400	5.92
3.5	12.6	30	15.4	450	5.50
3.7	12.6	35	15.0	500	5.14
4.0	12.6	40	14.7	600	4.55
4.2	12.6	45	14.4	700	4.07
4.5	12.7	50	14.3	800	3.69
5.0	12.8	60	13.8	900	3.37
6.0	13.2	70	13.3	1000	3.11
7.0	14.0	80	12.9		

basic *ab initio* structure and electron-scattering calculations, similar to those made for N_2O, were also performed for NO_2. The calculations using the Molpro suite, the MRCI (Multi-Reference Configuration Interaction) method, and the cc-pVTZ basis produced NO_2 properties that are in good agreement with the experimental values: The molecule has the C_{2v} geometry with the theoretical NO bond length of 1.184 Å and the bond angle of 134.4°. The experimental values[124] are 1.193 Å and 134.1° correspondingly. Theoretical rotational constants at the equilibrium geometry are 0.413, 8.08, and 0.435 cm^{-1}. The dipole moment is 0.302 D, while the reported experimental values are ranging in the interval 0.254–0.316 D (see Ref. 125 and references therein), with the positive charge displaced toward to the nitrogen atom corresponding to the polarity $O^-N^+O^-$. The electron-scattering calculations were performed using the theoretical values for the dipole moment and the equilibrium geometry. Previous experience suggests that it is safe to neglect the spin angular momentum when considering the rotational excitation of molecules with no overall orbital angular momentum.[126] The spin unresolved cross sections were computed using the UK R-matrix[88,89] and the POLYDCS[90] codes and are shown in Fig. 37.

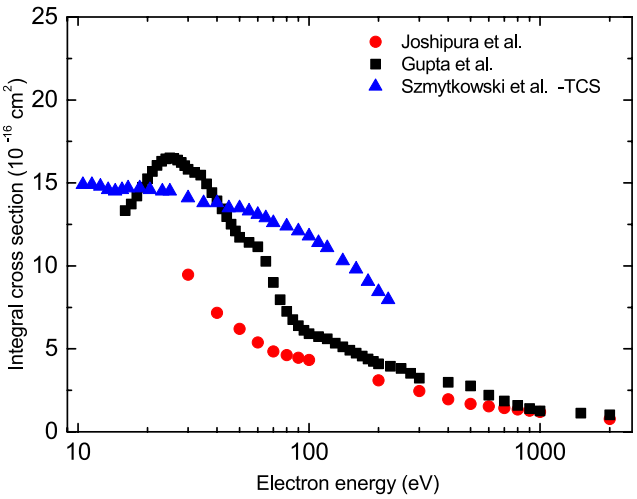

FIG. 35. Recommended elastic ICS of Joshipura *et al.*[122] compared with the values computed by Gupta *et al.*[120] and TCS measured by Szmytkowski *et al.*[119]

4.5. Vibrational excitation cross sections

There are no measured or theoretical data on the vibrational excitation of the NO_2 molecule by an electron impact. While

TABLE 17. Recommended elastic ICS and uncertainties (δ) for NO_2 in units of 10^{-16} cm^2. Energy in eV

Electron	ICS	Energy	ICS
30	9.47	300	2.46
40	7.17	400	1.96
50	6.21	500	1.68
60	5.39	600	1.54
70	4.85	700	1.43
80	4.62	800	1.34
90	4.47	900	1.27
100	4.33	1000	1.20
200	3.11	2000	0.77

Published by AIP Publishing on behalf of the National Institute of Standards and Technology.

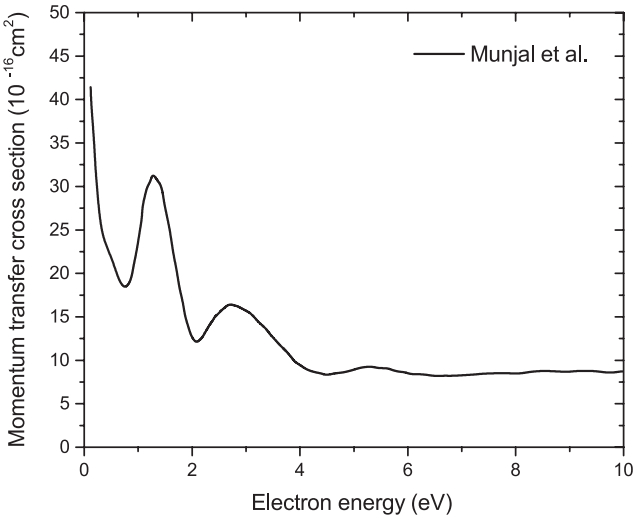

FIG. 36. Momentum transfer cross section of the NO_2 molecule computed using the R-matrix method by Munjal *et al.*[123]

experimental measurements of cross sections for the process could be long and expensive, a theoretical determination with a reasonable uncertainty seems to be a relatively straightforward problem for theorists working in the area of electron-molecule scattering.

4.6. Electronic excitation cross section

Measurements of electron scattering at 0 angle,[127] which correspond to the photoabsorption cross section, yielded a broad band centered at 3.12 eV, attributed to the $4b_2 \rightarrow 6a_1(^2A_1 \rightarrow ^2B_2)$ and $6a_1 \rightarrow 2b_1$ ($^2A_1 \rightarrow ^2B_1$) transitions.

A second broad band with a maximum of the photoabsorption cross section amounting to 0.13×10^{-16} cm^2 (a factor 2 higher than for the C $^1\Pi$ state in N_2O) extending from 6.3 to 9.4 eV results from excitation of the unpaired electron in the $6a_1$ orbital to the $5b_2$ virtual valence and the $3s\sigma$, $3p\sigma$, and 3π Rydberg orbitals[127] at 8 eV and attributed to $4b_2 \rightarrow 7a_1$ ($^2A_1 \rightarrow ^2B_2$) and $1a_2 \rightarrow 2b_1$ ($^2A_1 \rightarrow ^2B_1$) transitions.

A sharp maximum of the photoabsorption cross section with the value of 0.44×10^{-16} cm^2 is centered at 9.7 eV (see Fig. 38).

We are not aware of measurements of electronic excitations to either optically allowed or forbidden states. Mundjal *et al.*[123] and Gupta *et al.*[120] used the molecular R-matrix codes,[88] in the latter case through the Quantemol-N interface,[89] to obtain low-energy elastic and electronic excitation cross sections. According to Gupta *et al.*, ICS for the excitation $X\,^1A_1 \rightarrow ^2B_1$ (3.0 eV excitation energy) shows a sharp peak of 1.0×10^{-16} cm^2 just above the threshold. The nature of the peak is unclear.

As part of this study, we performed electron-scattering calculations for electronic excitation using the UK R-matrix code. We used the same basis and orbital sets, the same equilibrium geometry as in the rotational excitation calculations described above. Our computed cross sections are shown in Fig. 39. The cross sections were calculated for one single geometry, and no Franck-Condon overlap between initial and final vibrational levels of the electric states was accounted for. Such results could be viewed as an approximation for the cross sections where a sum over possible final vibrational levels and an average over initial levels are evaluated. The excitation thresholds in the obtained results are vertical transition energies, which should also be interpreted as approximate values of excitation energies for vibronic transitions with the most favorable Franck-Condon factors.

4.7. Dissociation cross section

There are no measured or theoretical data on neutral dissociation of the NO_2 molecule by an electron impact.

4.8. Ionization cross section

In spite of the importance of NO_2 in technological plasmas and its role as a precursor of the pollutant ozone formation in urban smog, ionization cross sections were studied in detail only in this century.

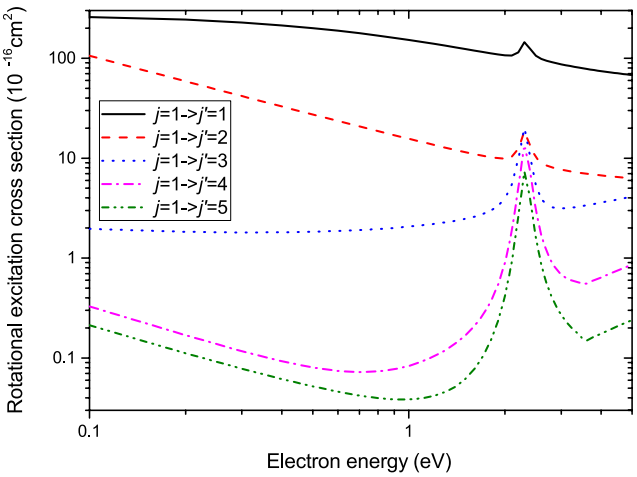

FIG. 37. Rotational excitation cross sections of the NO_2 molecule computed in this study.

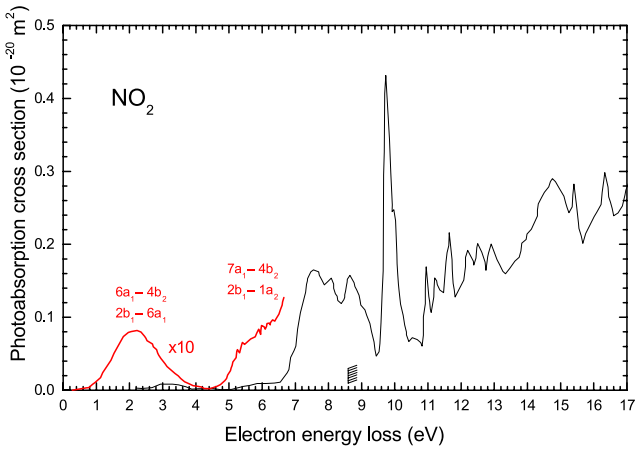

FIG. 38. Zero-angle electron-scattering energy loss spectra in NO_2 from experiments by Au *et al.*[127] The ionization threshold is 9.586 ± 0.002 eV for NO_2.

Published by AIP Publishing on behalf of the National Institute of Standards and Technology.

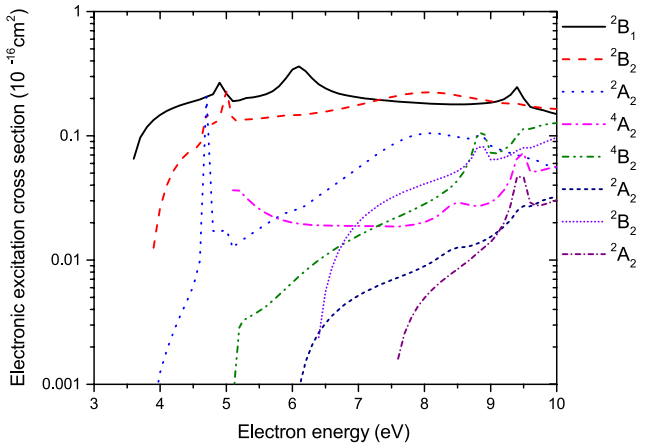

FIG. 39. Suggested cross sections electronic excitation of the NO_2 molecule from the ground state X^2A_1 into a few first excited states obtained in this study using the UK R-matrix[88,89] code.

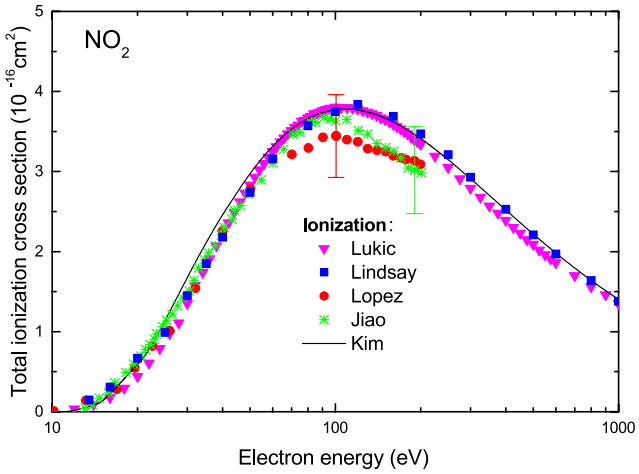

FIG. 40. Total ionization cross section in NO_2: gross total—Lukić *et al.*,[121] counting total—Jiao *et al.*,[128] Lindsay *et al.*,[29] and Lopez *et al.*[31] BEB model by Kim *et al.*[67] Recommended data are those by Lindsay *et al.*[29]

Lukić *et al.*[121] used a parallel plate ionization chamber. Thanks to a precise determination of the pressure in the scattering chamber, the gross total ionization cross section was measured up to 1000 eV with ±5% precision. Jiao *et al.*[128] used a Fourier-transform mass spectrometer, with a cubic trapping cell (5 cm on a side); the uncertainty on the absolute data was ±18%. They evaluated a fraction of doubly charged ions as less than 0.2% of the total ion population; they also proved that NO_2^+ and NO^+ ions are produced with thermal kinetic energies while recoil energies of O^+ and N^+ ions are less than 4.6 eV. All measurements[29,31,121,128] agree within the declared error bar; in particular, those by Lindsay *et al.*[29] agree with Lukić *et al.*[121] (and with BEB model[67]) within 5%, in the whole energy range between 50–1000 eV (see Fig. 40). Relatively good agreements also exist for partial cross sections. The dominant channel is the formation of the NO^+ dissociated ion (see Fig. 41). The three recent experiments[29,31,128] agree within combined error bars for the formation of both NO_2^+ and NO^+. Experimental NO_2^+ cross sections from Innsbruck[64] are lower by a factor of two than other experimental sets and are not shown in Fig. 41. Stephan *et al.*[64] also reported the formation of NO_2^{2+} ions, with the cross section three orders of magnitude lower than NO_2^+. In addition, partial cross sections for the formation of atomic ion fragments, O^+ (dominating) and N^+ from Lindsay *et al.*[29] and Jiao *et al.*,[128] agree well, within combined error bars (which are 15% and 20%, for the two ions, respectively, in the experiment of Lindsay *et al.*). The uncertainty on the combined ($N^+ + O^+$) yield is only 5% in that[29] experiment; the unresolved results of Lopez *et al.*[31] and the summed results of Jiao *et al.*[128] agree within error bars with Lindsay *et al.* (see Fig. 42). Our recommended set of NO_2 ionization coincides with that from the review by Lindsay and Mangan[27] and is based on measurements by Lindsay *et al.*[29] (see Table 18, Fig. 43).

4.9. Electron attachment (DEA) cross section

The work of Rangwala *et al.*[129] is the only report that presents the absolute DEA cross sections to the NO_2 molecule. In their experiment, a magnetically collimated and pulsed electron beam of variable energy is crossed with an effusive molecular beam producing negative ions. They reported the absolute cross section for the formation of O^- from NO_2 by DEA in the energy range from 0.0 eV to 5.4 eV. The resonance peaks were observed at the incident electron energies of 1.4, 3.1, and 8.3 eV. The numerical and graphical forms of the cross sections are given in Table 19 and Fig. 44, respectively. 1σ uncertainty at the peak cross section is 13%. Earlier than this, Abouf *et al.*[130] studied ions produced by dissociative attachment in NO_2 using a trochoidal monochromator as electron gun. O^-, O_2^-, and NO^- were observed. O^- production was much more dominant over O_2^- and NO^- ions. For O^- production, three peaks were observed with their maxima near 1.8 eV, 3.5 eV, and 8.5 eV, and the 1.8 eV peak is the most intense. These facts agree reasonably well with the result of

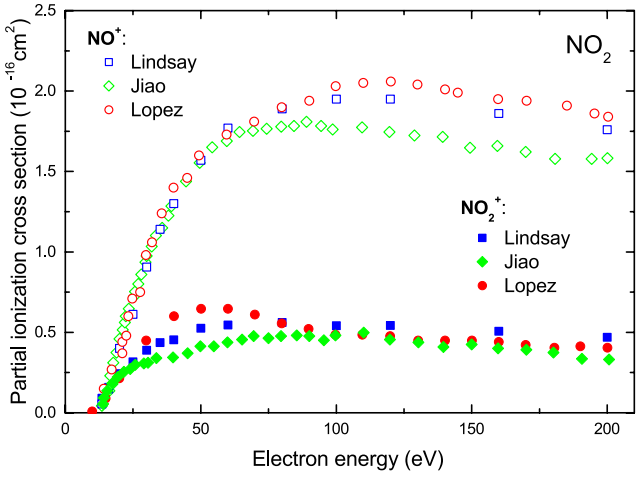

FIG. 41. Partial ionization cross sections in NO_2: lower, full points—formation of the NO_2^+ parent ion; upper, open points—formation of the NO^+ dissociated ion. Experiments by Jiao *et al.*,[128] Lindsay *et al.*,[29] and Lopez *et al.*[31] Recommended data are those by Lindsay *et al.*[29]

Published by AIP Publishing on behalf of the National Institute of Standards and Technology.

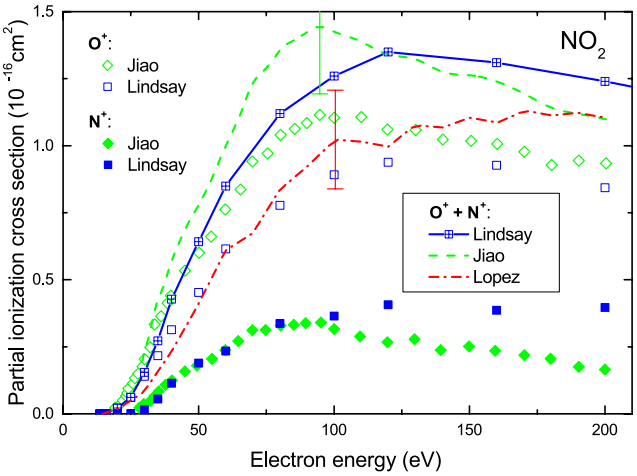

FIG. 42. Partial ionization of NO_2 into N^+ (lower, full points), O^+ (upper, open points), and nonresolved ($N^+ + O^+$)—lines. Experimental data from Refs. 29, 31, and 128.

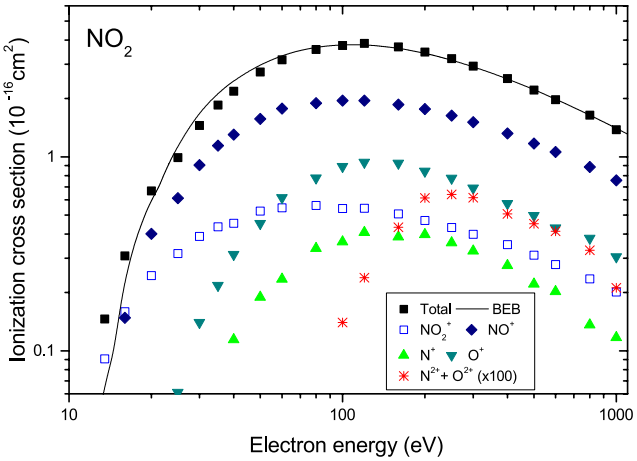

FIG. 43. Recommended cross sections for ionization of NO_2 are based on Lindsay *et al.*[29] measurements and are the same as given by Lindsay and Mangan in their review.[27] BEB model by Kim *et al.*[67] The uncertainties are ±5% on total ionization, NO_2^+, NO^+, and combined ($N^+ + O^+$) partial ionization cross sections, and ±20%, ±15%, and ±12% on N^+, O^+, and combined ($N^{2+} + O^{2+}$) partial ionizations, respectively.[27]

Rangwala *et al.*[129] However, Abouf *et al.*[130] did not report the absolute cross sections and did the measurements only in the limited electron-energy range.

5. Summary

In spite of being constituted of the same two elements, oxygen nitrides show significantly different features, as seen in electron

TABLE 18. Recommended cross sections for ionization of NO_2 are based on Lindsay *et al.*[29] measurements and are the same as given by Lindsay and Mangan in their review[27] in units of 10^{-16} cm^2. Energy in eV

Electron energy	CS NO_2^+	CS NO^+	CS N^+	CS O^+	CS N^{2+}+O^{2+}	CS total
13.5	0.0909	0.055	0	0	0	0.146
16	0.159	0.148	0	0	0	0.308
20	0.244	0.401	0	0.022	0	0.667
25	0.317	0.612	0	0.061	0	0.990
30	0.389	0.906	0.015	0.140	0	1.45
35	0.436	1.14	0.055	0.217	0	1.85
40	0.454	1.30	0.114	0.314	0	2.18
50	0.525	1.57	0.189	0.453	0	2.74
60	0.546	1.77	0.234	0.615	0	3.16
80	0.561	1.89	0.337	0.778	0	3.57
100	0.542	1.95	0.365	0.892	0.001 40	3.75
120	0.543	1.95	0.407	0.938	0.002 38	3.84
160	0.507	1.86	0.386	0.927	0.004 33	3.69
200	0.470	1.76	0.397	0.843	0.006 14	3.47
250	0.432	1.63	0.360	0.776	0.006 40	3.21
300	0.399	1.51	0.327	0.690	0.006 15	2.93
400	0.353	1.32	0.275	0.574	0.005 07	2.53
500	0.311	1.17	0.221	0.498	0.004 52	2.21
600	0.278	1.06	0.202	0.429	0.004 13	1.97
800	0.235	0.886	0.136	0.380	0.003 30	1.64
1000	0.201	0.756	0.117	0.305	0.002 11	1.38

TABLE 19. Recommended dissociative attachment cross sections (CS's) for the formation of O^- from NO_2 in units of 10^{-18} cm^2. Energy in eV

Energy	CS	Energy	CS
0.0	4.02	5.6	0.51
0.2	3.86	5.8	0.46
0.4	3.69	6.0	0.49
0.6	3.90	6.2	0.55
0.8	5.32	6.4	0.63
1.0	7.42	6.6	0.71
1.2	9.47	6.8	0.76
1.4	10.20	7.0	0.87
1.6	9.40	7.2	0.99
1.8	6.89	7.4	1.19
2.0	4.30	7.6	1.41
2.2	3.27	7.8	1.57
2.4	3.04	8.0	1.84
2.6	3.41	8.2	2.08
2.8	3.70	8.4	1.99
3.0	3.96	8.6	1.92
3.2	3.96	8.8	1.69
3.4	3.70	9.0	1.58
3.6	3.25	9.2	1.24
3.8	3.03	9.4	1.11
4.0	2.27	9.6	0.95
4.2	1.90	9.8	0.82
4.4	1.48	10.0	0.83
4.6	0.99	10.2	0.76
4.8	0.87	10.4	0.71
5.0	0.62	10.6	0.79
5.2	0.52	10.8	0.79
5.4	0.45	11.0	0.76

Published by AIP Publishing on behalf of the National Institute of Standards and Technology.

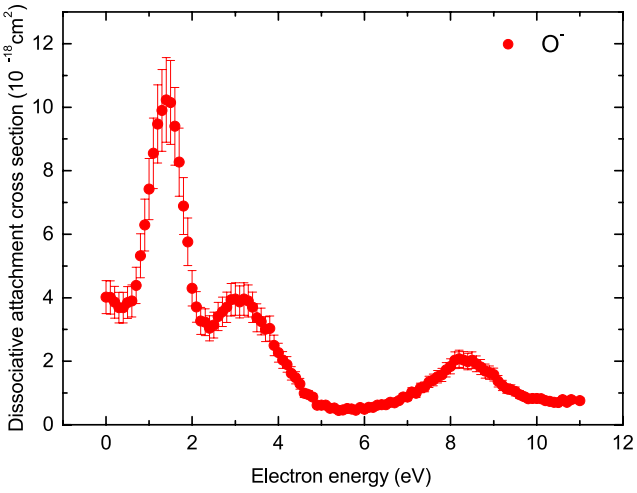

FIG. 44. Recommended cross sections for the formation of O^- from NO_2.

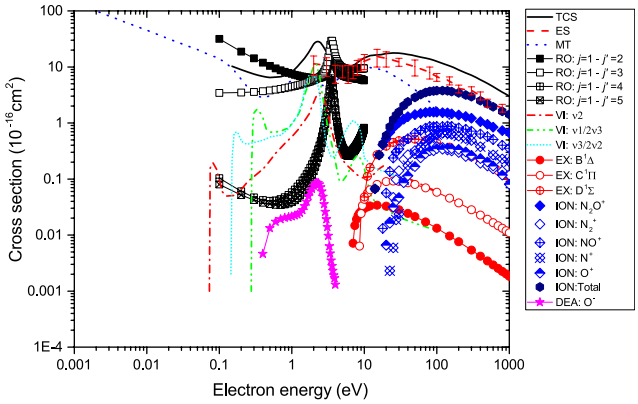

FIG. 46. Summary of the recommended cross section for electron collisions with N_2O. TCS—total scattering, ES—elastic scattering, MT—momentum transfer, ION—ionization, VI—vibrational excitation, RO—rotational excitation, EX—electronic excitation, and DEA—dissociative electron attachment.

scattering. Biologically, NO, N_2O, and NO_2 are drastically different. NO, which is formed in nostrils during breathing, contributes to better oxygenation of the blood; N_2O is slightly anesthetic, while NO_2 is poisonous.

Figures 45–47 summarize our recommended electron collision cross sections for NO, N_2O, and NO_2, respectively. The most prominent feature for NO at 1 eV and below are two overlapping resonances, giving rise to a structure visible in TCS as a series of sharp peaks: in this, the NO molecule resembles O_2.[13] The TCS in N_2O shows a broad resonant peak, which in the vibrational channel constitutes one-third of the TCS at 2.3 eV (see Fig. 46).

In the recommended TCS's, the rotational structure is not resolved. Therefore, the recommended TCS's should be understood as summed over all possible final rotational states and averaged over initial states of the target molecule for the energy distribution of the experiments in which the cross sections were measured. For example, the rotational excitation cross sections shown in Figs. 46 and 47 are state-selective and could be larger for certain transitions than the TCS's with unresolved rotational structure.

In NO_2, which is also a "prototype" system showing similar features to ozone, theory[123] predicts two narrow resonances at 1–3 eV (see Fig. 36). They are clearly visible in the dissociative attachment channel and as an enhancement of the rotational-excitation cross sections at about 2.2 eV, as predicted by the present theory (see Fig. 37).

Electronic excitation in the open shell NO molecule shows a number of partially overlapping states, starting from some 4.75 eV; in N_2O, it is dominated by two dipole-allowed states, visible as broad peaks, centered at 8.5 eV and 9.5 eV in the energy-loss spectra. In their maxima, the electronic excitation cross sections amount to about 3% of the TCS. A similar proportion is predicted by the present R-matrix calculation for NO_2 in the energy range 9–10 eV (see Fig. 39).

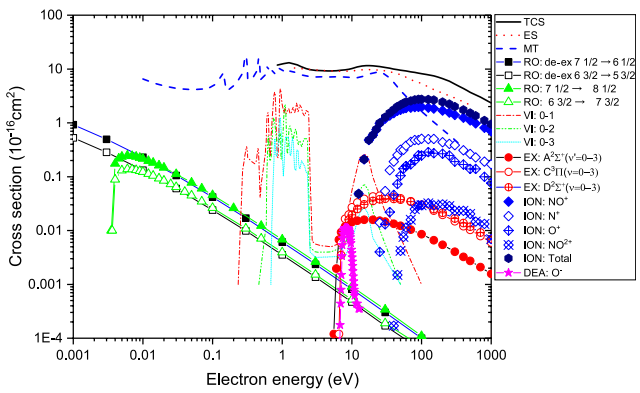

FIG. 45. Summary of the recommended cross section for electron collisions with NO. TCS—total scattering, ES—elastic scattering, MT—momentum transfer, ION—ionization, VI—vibrational excitation, RO—rotational excitation, EX—electronic excitation, and DEA—dissociative electron attachment.

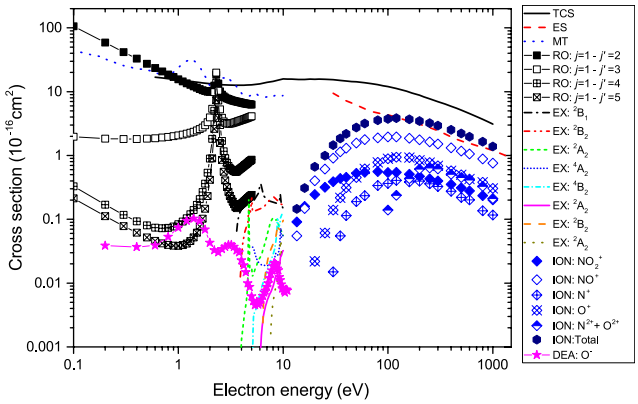

FIG. 47. Summary of the recommended cross section for electron collisions with NO_2. TCS—total scattering, ES—elastic scattering, MT—momentum transfer, ION—ionization, RO—rotational excitation, EX—electronic excitation, and DEA—dissociative electron attachment.

Published by AIP Publishing on behalf of the National Institute of Standards and Technology.

Comparing the ionization cross sections for the three nitrogen oxides, the total ionization cross sections scale roughly with molecular dipole polarizabilities.[131] The total ionization cross sections in NO_2 and N_2O practically coincide, amounting in their maxima, respectively, to 3.84 and 3.77 $\times$ 10^{-16} cm^2 (with respective polarizabilities, 2.91 and 2.998 $\times$ 10^{-30} m^2, see Table 1). Total ionization cross sections are well reproduced by the BEB model[32,67] for all three nitrogen oxides. The optical potential model[122] overestimates slightly (10%–15%) the total ionization cross sections for all three targets. Figure 48 compares partitioning into different channels of ionization at 100 eV and 1000 eV. For neither N_2O nor NO_2, the parent ion is the dominant product (i.e., constitutes over 50% of the ionization events) at energies where other channels are available. The NO^+ dissociated ion is the main ion in the ionization of NO_2 and constitutes about $\frac{1}{4}$ of ionization events in of N_2O. The N^+ ion is formed with roughly double the probability of the O^+ ion in NO and N_2O; in NO_2, the O^+ ion prevails over N^+ (see Fig. 48).

In summary, the main differences between the three nitrogen oxides are visible in the low energy range (below 5 eV) where the cross sections display the existence of different resonances. This energy region is the one for which biological processes are influenced the most. Experimental (and theoretical) studies are still needed. In particular, our knowledge on electron scattering is broadly satisfactory for NO and N_2O, but it has many gaps for NO_2: for example, we are not aware of measurements of the vibrational or electronic-excitation cross sections. For NO and NO_2, we also lack measurements of dissociation into neutrals.

Acknowledgments

We thank Tom Meltzer for providing the data for Fig. 1. This work was supported by the R&D Program of "Plasma BigData ICT Convergence Technology Research Project" through the National Fusion Research Institute of Korea (NFRI) funded by the Government funds. This work was partly supported by the Technology Innovation Program (No. 20003641, Development and Dissemination on National Standard Reference Data) funded by the Ministry of Trade, Industry & Energy (MOTIE, Korea). V.K. acknowledges the support from the National Science Foundation (Grant No. PHY-1806915).

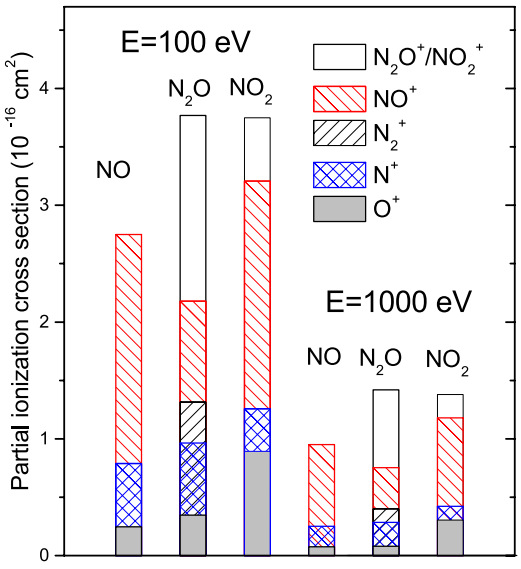

FIG. 48. Partial ionization cross sections in NO, N_2O, and NO_2. Data are from recommended sets (see text).

6. Appendix: Electron Swarm Parameters in Pure NO and NO-Ar Mixtures

The drift velocity and the product of the gas number density and the longitudinal diffusion coefficient (ND_L) in pure NO and in the 4.99% NO-Ar mixture were measured by Takeuchi and Nakamura[43] and re-analyzed here (Figs. 49–51). These swarm parameters were determined differentially from arrival-time distributions (ATDs) of an isolated electron pulse observed at several drift distances from the cathode at each E/N (E is the electric field strength and N is the gas number density, 1 Td = 14 $\times 10^{-17}$ Vcm^2) by using the double shutter electron drift tube with a variable drift distance (1–10 cm). The purity of NO was 99.99%, and the mix-ratio was measured by a gas-chromatograph of the gas company. At low E/N (<10 Td) in pure NO, the ATD of electrons decays rapidly with the distance due to the three-body attachment process in NO.[132] The ATD has also increased at its later time showing there are delayed electron components, which possibly are electrons autodetached from unstable negative ions. This increase deteriorates the observed ATD substantially and gives rise to the apparent gas-density dependence of the swarm parameters, especially of ND_L. The gas density-independent drift velocity was estimated through the extrapolation to N = 0. This probably is the reason of scattering results of earlier drift velocity measurements.[133,134] In NO–Ar mixtures, on the other hand, the ATD at high E/N (>50 Td) shows strong growth with the drift distance, probably due to the Penning ionization, and it was not possible to determine swarm parameters properly. The magnitude of the drift velocity around the maximum (2.5 Td) and the minimum (10 Td) depends on

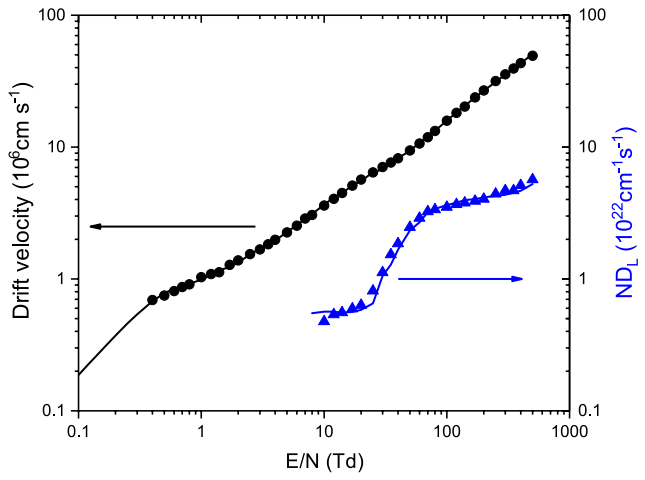

FIG. 49. The drift velocity and ND_L of electrons in pure NO. Solid circle, electron drift velocity; solid triangle, ND_L; solid line, Boltzmann equation calculation using the present recommended cross section set of NO.

Published by AIP Publishing on behalf of the National Institute of Standards and Technology.

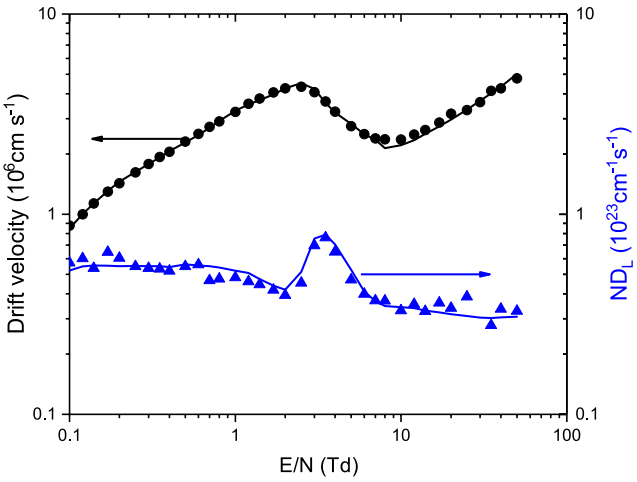

FIG. 50. The drift velocity and ND_L of electrons in the 4.99% NO–Ar mixture. Solid circle, electron drift velocity; solid triangle, ND_L,; solid line, Boltzmann equation calculation using the present recommended cross section set of NO.

the magnitude of vibrational cross sections and the threshold magnitude of the electron excitation cross section, respectively. The magnitude and width of the prominent peak structure seen in the ND_L depends on the depth and width of the minimum of the inelastic cross section of NO over 2.5–7 eV range. Lakshminarasimha and Lucas[135] measured the ionization coefficient in NO over the E/N range 56–1412 Td with the accuracy of ±3%. In order that the measured ionization coefficient can be reproduced within the claimed accuracy by a Boltzmann equation analysis, the sum of the electronic excitation cross sections should be larger than the sum of Brunger *et al.*[50] by a factor of about 5, as shown in Fig. 13.

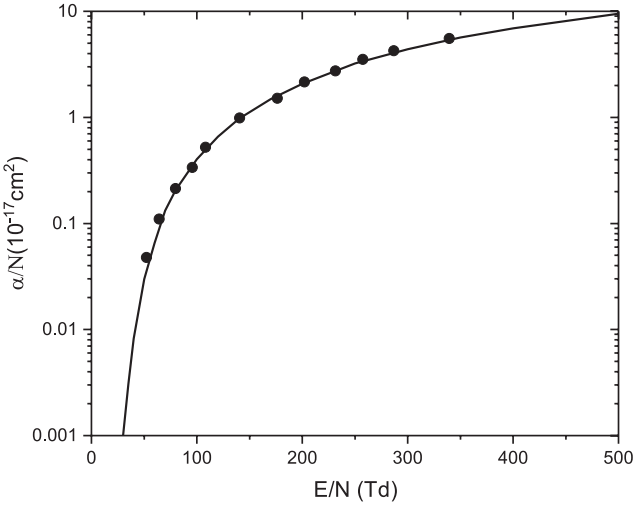

FIG. 51. The ionization coefficient of NO. Solid circle, experimental result; solid line, Boltzmann equation calculation using the present recommended cross section set of NO.

7. References

[1]M.-Y. Song, J. S. Yoon, H. Cho, Y. Itikawa, G. P. Karwasz, V. Kokoouline, Y. Nakamura, and J. Tennyson, "Cross sections for electron collisions with methane," J. Phys. Chem. Ref. Data **44**, 023101 (2015).

[2]M.-Y. Song, J.-S. Yoon, H. Cho, G. P. Karwasz, V. Kokoouline, Y. Nakamura, and J. Tennyson, "Cross sections for electron collisions with acetylene," J. Phys. Chem. Ref. Data **46**, 013106 (2017).

[3]M.-Y. Song, J.-S. Yoon, H. Cho, G. P. Karwasz, V. Kokoouline, Y. Nakamura, J. R. Hamilton, and J. Tennyson, "Cross sections for electron collisions with NF_3," J. Phys. Chem. Ref. Data **46**, 043104 (2017).

[4]R. Zhang, A. Faure, and J. Tennyson, "Electron and positron collisions with polar molecules: Studies with the benchmark water molecule," Phys. Scr. **80**, 015301 (2009).

[5]R. J. Hargreaves, I. E. Gordon, L. S. Rothman, S. A. Tashkun, V. I. Perevalov, A. A. Lukashevskaya, S. N. Yurchenko, J. Tennyson, and H. S. Müller, "Spectroscopic line parameters of NO, NO_2, and N_2O for the hitemp database," J. Quant. Spectrosc. Radiat. Transfer **232**, 35–53 (2019).

[6]R. D. Nelson, Jr., D. R. Lide, and A. A. Maryott, *Selected Values of Electric Dipole Moments for Molecules in the Gas Phase*, NSRDS-NBS10 (U.S. Department of Commerce, National Bureau Standards, Washington, DC, 1967).

[7]T. N. Olney, N. Cann, G. Cooper, and C. Brion, "Absolute scale determination for photoabsorption spectra and the calculation of molecular properties using dipole sum-rules," Chem. Phys. **223**, 59–98 (1997).

[8]M. J. Travers, D. C. Cowles, and G. Ellison, "Reinvestigation of the electron affinities of O_2 and NO," Chem. Phys. Lett. **164**, 449–455 (1989).

[9]E. S. Kryachko, C. Vinckier, and M. T. Nguyen, "Another look at the electron attachment to nitrous oxide," J. Chem. Phys. **114**, 7911–7917 (2001).

[10]K. M. Ervin, J. Ho, and W. C. Lineberger, "Ultraviolet photoelectron spectrum of nitrite anion," J. Phys. Chem. **92**, 5405–5412 (1988).

[11]*CRC Handbook of Chemistry and Physics*, 96th ed., edited by W. M. Haynes (CRC Press, Boca Raton, FL, 2015), Vol. 96.

[12]A. Wong, S. N. Yurchenko, P. Bernath, H. S. P. Mueller, S. McConkey, and J. Tennyson, "ExoMol line list XXI: Nitric oxide (NO)," Mon. Not. R. Astron. Soc. **470**, 882–897 (2017).

[13]G. P. Karwasz, R. S. Brusa, and A. Zecca, "Total scattering cross sections: Datasheet from Landolt-Börnstein," in *Interactions of Photons and Electrons with Molecules*, Group I Elementary Particles, Nuclei and Atoms, edited by Y. Itikawa (Springer-Verlag, Berlin, Heidelberg, 2003), Vol. 17, Chap. 6.1.

[14]K. Anzai, H. Kato, M. Hoshino, H. Tanaka, Y. Itikawa, L. Campbell, M. J. Brunger, S. J. Buckman, H. Cho, F. Blanco, G. Garcia, P. Limão-Vieira, and O. Ingólfsson, "Cross section data sets for electron collisions with H_2, O_2, CO, CO_2, N_2O and H_2O," Eur. Phys. J. D **66**, 36 (2012).

[15]A. Zecca, G. P. Karwasz, R. S. Brusa, and T. Wroblewski, "Low-energy electron collisions in nitrogen oxides: A comparative study," Int. J. Mass Spectrom. **223-224**, 205–215 (2003).

[16]Y. Itikawa, "Cross sections for electron collisions with nitric oxide," J. Phys. Chem. Ref. Data **45**, 033106 (2016).

[17]E. Brüche, "Wirkungsquerschnitt und Molekülbau," Ann. Phys. **388**, 1065–1128 (1927).

[18]A. Zecca, I. Lazzizzera, M. Krauss, and C. E. Kuyatt, "Electron scattering from NO and N_2O below 10 eV," J. Chem. Phys. **61**, 4560–4566 (1974).

[19]G. Dalba, P. Fornasini, R. Grisenti, G. Ranieri, and A. Zecca, "Absolute total cross section measurements for intermediate energy electron scattering. II. N_2, O_2 and NO," J. Phys. B: At. Mol. Phys. **13**, 4695–4701 (1980).

[20]C. Szmytkowski and K. Maciag, "Total cross section for electron impact on nitrogen monoxide," J. Phys. B: At. Mol. Phys. **24**, 4273–4279 (1991).

[21]C. Szmytkowski, K. Maciag, and G. Karwasz, "Absolute electron scattering total cross section measurements for noble gas atoms and diatomic molecules," Phys. Scr. **54**, 271–280 (1996).

[22]D. T. Alle, M. J. Brennan, and S. J. Buckman, "Low-energy total electron scattering cross section and electron affinity for NO," J. Phys. B: At., Mol. Opt. Phys. **29**, L277–L282 (1996).

[23]M. Allan, "Transitions between the $^2\Pi_{1/2}$ and $^2\Pi_{3/2}$ spin-orbit components of NO induced by impact of slow electrons," Phys. Rev. Lett. **93**, 063201 (2004).

Published by AIP Publishing on behalf of the National Institute of Standards and Technology.

[24]M. Allan, "Electron collisions with NO: Elastic scattering, vibrational excitation and $^2\Pi_{1/2} \rightleftharpoons {}^2\Pi_{1/2}$ transitions," J. Phys. B: At., Mol. Opt. Phys. **38**, 603–614 (2005).
[25]L. Josić, T. Wróblewski, Z. L. Petrović, J. Mechlińska-Drewko, and G. Karwasz, "Influence of resonant scattering on electron-swarm parameters in NO," Chem. Phys. Lett. **350**, 318–324 (2001).
[26]G. Karwasz, R. Brusa, A. Gasparoli, and A. Zecca, "Total cross-section measurements for e^-—CO scattering: 80–4000 eV," Chem. Phys. Lett. **211**, 529–533 (1993).
[27]B. G. Lindsay and M. A. Mangan, "Ionization: Datasheet from Landolt-Börnstein," in *Interactions of Photons and Electrons with Molecules*, Group I Elementary Particles, Nuclei and Atoms, edited by Y. Itikawa (Springer-Verlag, Berlin, Heidelberg, 2003), Vol. 17, Chap 5.1.
[28]D. Rapp and P. Englander-Golden, "Total cross sections for ionization and attachment in gases by electron impact. I. Positive ionization," J. Chem. Phys. **43**, 1464–1479 (1965).
[29]B. G. Lindsay, M. A. Mangan, H. C. Straub, and R. F. Stebbings, "Absolute partial cross sections for electron-impact ionization of NO and NO_2 from threshold to 1000 eV," J. Chem. Phys. **112**, 9404–9410 (2000).
[30]I. Iga, M. V. V. S. Rao, and S. K. Srivastava, "Absolute electron impact ionization cross sections for N_2O and NO from threshold up to 1000 eV," J. Geophys. Res. E **101**, 9261–9266 (1996).
[31]J. Lopez, V. Tarnovsky, M. Gutkin, and K. Becker, "Electron-impact ionization of NO, NO_2, and N_2O," Int. J. Mass Spectrom. **225**, 25–37 (2003).
[32]W. Hwang, Y. Kim, and M. E. Rudd, "New model for electron-impact ionization cross sections of molecules," J. Chem. Phys. **104**, 2956–2966 (1996).
[33]C. K. Kwan, Y. F. Hsieh, W. E. Kauppila, S. J. Smith, T. S. Stein, M. N. Uddin, and M. S. Dababneh, "Total-scattering measurements and comparisons for collisions of electrons and positrons with N_2O," Phys. Rev. Lett. **52**, 1417–1420 (1984).
[34]C. Szmytkowski, P. Możejko, and G. Kasperski, "Electron scattering on triatomic molecules: SO_2, OCS and N_2O," in *Proceedings of the XVIII International Symposium on Physics of Ionized Gases*, edited by B. Vujicic and S. Djurovic (Faculty of Sciences, Institute of Physics Novi Sad, Kotor, Yugoslavia, 1996), pp. 66–69.
[35]X. Shilin, Z. Fang, Y. Liqiang, Y. Changqing, and X. Kezun, "Absolute total cross section measurement for electron scattering on N_2O in the energy range 600–4250 eV," J. Phys. B: At., Mol. Opt. Phys. **30**, 2867–2871 (1997).
[36]A. Zecca, J. C. Nogueira, G. P. Karwasz, and R. S. Brusa, "Total cross sections for electron scattering on NO_2, OCS, SO_2 at intermediate energies," J. Phys. B: At., Mol. Opt. Phys. **28**, 477–486 (1995).
[37]B. Mojarrabi, R. J. Gulley, A. G. Middleton, D. C. Cartwright, P. J. O. Teubner, S. J. Buckman, and M. J. Brunger, "Electron collisions with NO: Elastic scattering and rovibrational (0 to 1, 2, 3, 4) excitation cross sections," J. Phys. B: At., Mol. Opt. Phys. **28**, 487–504 (1995).
[38]M. Jelisavcic, R. Panajotovic, and S. J. Buckman, "Absolute collision cross sections for low energy electron scattering from NO: The role of resonances in elastic scattering and vibrational excitation," Phys. Rev. Lett. **90**, 203201 (2003).
[39]M. J. Brunger, L. Campbell, D. C. Cartwright, A. G. Middleton, B. Mojarrabi, and P. J. O. Teubner, "Electron-impact excitation of Rydberg and valence electronic states of nitric oxide: II. Integral cross sections," J. Phys. B: At., Mol. Opt. Phys. **33**, 809–819 (2000).
[40]M. M. Fujimoto and M. T. Lee, "Elastic and absorption cross sections for electron-nitric oxide collisions," J. Phys. B: At., Mol. Opt. Phys. **33**, 4759–4768 (2000).
[41]Y. Itikawa, "Momentum-transfer cross sections for electron collisions with atoms and molecules," At. Data Nucl. Data Tables **14**, 1–10 (1974).
[42]A. V. Phelps and JILA, *Compilation of Electron Cross Sections* (University of Colorado, Colorado, 1995).
[43]T. Takeuchi and Y. Nakamura, "Electron collision cross section set for NO molecules via electron swarm study," The Papers of Technical Meeting on Electrical Discharges IEE Jpn. **ED-02-95**, 53–57 (2002).
[44]Y. Itikawa and N. Mason, "Rotational excitation of molecules by electron collisions," Phys. Rep. **414**, 1–41 (2005).
[45]K. Takayanagi, "Rotational and vibrational excitation of polar molecules by slow electrons," J. Phys. Soc. Jpn. **21**, 507–514 (1966).
[46]D. E. Stogryn and A. P. Stogryn, "Molecular multipole moments," Mol. Phys. **11**, 371–393 (1966).
[47]T. Takeuchi and Y. Nakamura, "Measurements of electron transport coefficients in pure NO and in NO–Ar mixtures," Trans. IEE Jpn. **121-A**, 481–486 (2001).
[48]L. Campbell, M. J. Brunger, Z. L. Petrovic, M. Jelisavcic, R. Panajotovic, and S. J. Buckman, "Infrared auroral emissions driven by resonant electron impact excitation of NO molecules," Geophys. Res. Lett. **31**, L10103 (2004).
[49]L. C. Pitchford, L. L. Alves, K. Bartschat, S. F. Biagi, M.-C. Bordage, I. Bray, C. E. Brion, M. J. Brunger, L. Campbell, A. Chachereau, B. Chaudhury, L. G. Christophorou, E. Carbone, N. A. Dyatko, C. M. Franck, D. V. Fursa, R. K. Gangwar, V. Guerra, P. Haefliger, G. J. M. Hagelaar, A. Hoesl, Y. Itikawa, I. V. Kochetov, R. P. McEachran, W. L. Morgan, A. P. Napartovich, V. Puech, M. Rabie, L. Sharma, R. Srivastava, A. D. Stauffer, J. Tennyson, J. de Urquijo, J. van Dijk, L. A. Viehland, M. C. Zammit, O. Zatsarinny, and S. Pancheshnyi, "LXCat: An Open-access, web-based platform for data needed for modeling low temperature plasmas," Plasma Proc. Polym. **14**, 1600098 (2017).
[50]M. J. Brunger, L. Campbell, D. C. Cartwright, A. G. Middleton, B. Mojarrabi, and P. J. O. Teubner, "Electron-impact excitation of Rydberg and valence electronic states of nitric oxide: I. differential cross sections," J. Phys. B: At., Mol. Opt. Phys. **33**, 783–808 (2000).
[51]W. F. Chang, G. Cooper, and C. E. Brion, "Absolute optical oscillator strengths for the photoabsorption of nitric oxide (5–30 eV) at high resolution," Chem. Phys. **170**, 111–121 (1993).
[52]L. E. Machado, A. L. Monzani, M.-T. Lee, and M. M. Fujimoto, in *Proceedings of the International Symposium on Electron- and Photon- Molecule Collisions and Swarms* (Lawrence Livermore Press, Berkeley, CA, 1995), p. H32.
[53]H. Kato, H. Kawahara, M. Hoshino, H. Tanaka, and M. J. Brunger, "Excitation of the $A^2\Sigma^+$, $C^2\Pi$ and $D^2\Sigma^+$ Rydberg-electronic states in NO by 100 eV electrons," Chem. Phys. Lett. **444**, 34–38 (2007).
[54]V. V. Skubenich, M. M. Povch, and I. P. Zapesochnyi, "Excitation of diatomic molecules on collisions with monoenergetic electrons," Khimiya Vysokikh Energii **11**, 116–123 (1977) (in Russian).
[55]R. S. Schappe, R. J. Edgell, and E. Urban, "Electron-impact excitation of nitric oxide ($A^2\Sigma^+ - X^2\Pi$)," Phys. Rev. A **65**, 042701 (2002).
[56]X. Xu, L.-Q. Xu, T. Xiong, T. Chen, Y.-W. Liu, and L.-F. Zhu, "Oscillator strengths and integral cross sections for the valence-shell excitations of nitric oxide studied by fast electron impact," J. Chem. Phys. **148**, 044311 (2018).
[57]Y.-K. Kim, "Scaling of plane-wave Born cross sections for electron-impact excitation of neutral atoms," Phys. Rev. A **64**, 032713 (2001).
[58]R. Olszewski and M. Zubek, "A study of electron impact excitation of the $A^2\Sigma^+$ state of nitric oxide in the near-threshold energy range," Chem. Phys. Lett. **340**, 249–255 (2001).
[59]M. Imami and W. L. Borst, "Electron impact excitation of the gamma bands of nitric oxide," J. Chem. Phys. **63**, 3602–3605 (1975).
[60]L. R. LeClair and J. W. McConkey, "Selective detection of $O(^1S_0)$ following electron impact dissociation of O_2 and N_2O using a XeO* conversion technique," J. Chem. Phys. **99**, 4566–4577 (1993).
[61]J. W. McConkey, C. P. Malone, P. V. Johnson, C. Winstead, V. McKoy, and I. Kanik, "Electron impact dissociation of oxygen-containing molecules—A critical review," Phys. Rep. **466**, 1–103 (2008).
[62]E. A. MacDonald, E. Donovan, Y. Nishimura, N. A. Case, D. M. Gillies, B. Gallardo-Lacourt, W. E. Archer, E. L. Spanswick, N. Bourassa, M. Connors, M. Heavner, B. Jackel, B. Kosar, D. J. Knudsen, C. Ratzlaff, and I. Schofield, "New science in plain sight: Citizen scientists lead to the discovery of optical structure in the upper atmosphere," Sci. Adv. **4**, eaaq0030 (2018).
[63]J. T. Tate and P. T. Smith, "The efficiencies of ionization and ionization potentials of various gases under electron impact," Phys. Rev. **39**, 270–277 (1932).
[64]K. Stephan, H. Helm, Y. B. Kim, G. Seykora, J. Ramler, M. Grössl, E. Märk, and T. D. Märk, "Single and double ionization of nitrogen dioxide by electron impact from threshold up to 180 eV," J. Chem. Phys. **73**, 303–308 (1980).
[65]E. Märk, T. D. Märk, Y. B. Kim, and K. Stephan, "Absolute electron impact ionization cross section from threshold up to 180 eV for $N_2O + e \rightarrow N_2O^+ + 2e$ and the metastable and collision induced dissociation of N_2O^+," J. Chem. Phys. **75**, 4446–4453 (1981).
[66]Y. B. Kim, K. Stephan, E. Märk, and T. D. Märk, "Single and double ionization of nitric oxide by electron impact from threshold up to 180 eV," J. Chem. Phys. **74**, 6771–6776 (1981).

Published by AIP Publishing on behalf of the National Institute of Standards and Technology.

[67]Y.-K. Kim, W. Hwang, N. M. Weinberger, M. A. Ali, and M. E. Rudd, "Electron-impact ionization cross sections of atmospheric molecules," J. Chem. Phys. **106**, 1026–1033 (1997).
[68]M. Kumar, Y. Kumar, N. Tiwari, and S. Tomar, "Total ionization cross sections of NO_2, CO and CS molecules due to electron impact," J. At. Mol. Sci. **4**, 30–40 (2013).
[69]D. Rapp and D. D. Briglia, "Total cross sections for ionization and attachment in gases by electron impact. II. Negative ion formation," J. Chem. Phys. **43**, 1480–1489 (1965).
[70]O. J. Orient and A. Chutjian, "Detection of new dissociative electron attachment channels in NO," Phys. Rev. Lett. **74**, 5017–5019 (1995).
[71]C. Ramsauer and R. Kollath, "Über den Wirkungsquerschnitt der Gasmolekule Gegenüber Elektronen unterhalb 1 Volt," Nachtrag, Ann. Phys. **7**, 176–182 (1930).
[72]C. Szmytkowski, G. Karwasz, and K. Maciag, "Absolute total electron-scattering cross sections of N_2O and OCS in the low-energy region," Chem. Phys. Lett. **107**, 481–484 (1984).
[73]B. Marinkovic, C. Szmytkowski, V. Pejcev, D. Filipovic, and L. Vuskovic, "Differential cross sections for elastic and inelastic scattering of electrons by N_2O in the range from 10 to 80 eV," J. Phys. B: At., Mol. Opt. Phys. **19**, 2365–2375 (1986).
[74]C. Szmytkowski, K. Maciag, G. Karwasz, and D. Filipovic, "Total absolute cross section measurements for electron scattering on NH_3, OCS and N_2O," J. Phys. B: At., Mol. Opt. Phys. **22**, 525–530 (1989).
[75]L. A. Morgan, C. J. Gillan, J. Tennyson, and X. Chen, "R-matrix calculations for polyatomic molecules: Electron scattering by N_2O," J. Phys. B: At., Mol. Opt. Phys. **30**, 4087–4096 (1997).
[76]C. Winstead and V. McKoy, "Electron collisions with nitrous oxide," Phys. Rev. A **57**, 3589–3597 (1998).
[77]G. P. Karwasz, T. Wróblewski, R. S. Brusa, and E. Illenberger, "Electron scattering on triatomic molecules: The need for data," Jpn. J. Appl. Phys. **45**, 8192–8196 (2006).
[78]W. M. Johnstone and W. R. Newell, "Absolute elastic cross sections for electron scattering from N_2O," J. Phys. B: At., Mol. Opt. Phys. **26**, 129–138 (1993).
[79]M. Kitajima, Y. Sakamoto, S. Watanabe, T. Suzuki, T. Ishikawa, H. Tanaka, and M. Kimura, "Absolute elastic differential cross-sections for electron scattering by N_2O at 1.5–100 eV," Chem. Phys. Lett. **309**, 414–420 (1999).
[80]M. Kitajima, Y. Sakamoto, R. J. Gulley, M. Hoshino, J. C. Gibson, H. Tanaka, and S. J. Buckman, "Electron scattering from N_2O: Absolute elastic scattering and vibrational excitation," J. Phys. B: At., Mol. Opt. Phys. **33**, 1687–1702 (2000).
[81]M.-T. Lee, I. Iga, M. G. P. Homem, L. E. Machado, and L. M. Brescansin, "Elastic and absorption cross sections for electron–nitrous oxide collisions," Phys. Rev. A **65**, 062702 (2002).
[82]J. L. Pack, R. E. Voshall, and A. V. Phelps, "Drift velocities of slow electrons in krypton, xenon, deuterium, carbon monoxide, carbon dioxide, water vapor, nitrous oxide, and ammonia," Phys. Rev. **127**, 2084–2089 (1962).
[83]Y. Singh, "Scattering cross sections for slow electrons in polyatomic gases," J. Phys. B: At. Mol. Phys. **3**, 1222–1231 (1970).
[84]F. T. O'Malley, "Extrapolation of electron-rare gas atom cross sections to zero energy," Phys. Rev. **130**, 1020–1029 (1963).
[85]M. Hayashi, *Handbook on Plasma Material Science* (Ohmsha, Tokyo, 1992), p. 759.
[86]Y. Nakamura, "Electron swarm parameters in pure N_2O and in dilute N_2O–Ar mixtures and electron collision cross sections of N_2O molecule," in *Proceedings of the 28th ICPIG*, edited by Y. Nakamura (Prague, Czech Republic, 2007).
[87]J. F. Nolan and A. V. Phelps, "Measurement of Cesium excitation cross section near threshold by a swarm technique," Phys. Rev. **140**, A792–A799 (1965).
[88]J. Carr, P. Galiatsatos, J. Gorfinkiel, A. Harvey, M. Lysaght, D. Madden, Z. Mašín, M. Plummer, J. Tennyson, and H. Varambhia, "UKRmol: A low-energy electron- and positron-molecule scattering suite," Euro. Phys. J. D **66**, 58 (2012).
[89]J. Tennyson, D. B. Brown, J. J. Munro, I. Rozum, H. N. Varambhia, and N. Vinci, "Quantemol-N: An expert system for performing electron molecule collision calculations using the R-matrix method," J. Phys. Conf. Series **86**, 012001 (2007).
[90]N. Sanna and F. A. Gianturco, "Differential cross sections for electron/positron scattering from polyatomic molecules," Comput. Phys. Commun. **114**, 142 (1998).
[91]K. Mogi, T. Komine, and K. Hirao, "A theoretical study on the dipole moment of N_2O and the weakly bound complexes formed by N_2O," J. Chem. Phys. **95**, 8999–9008 (1991).
[92]H. Jalink, D. H. Parker, and S. Stolte, "Experimental-verification of the sign of the electric-dipole moment of N_2O," J. Mol. Spectrosc. **121**, 236–237 (1987).
[93]J. M. L. J. Reinartz, W. L. Meerts, and A. Dymanus, "Hyperfine-structure, electric and magnetic-properties of $^{14}N_2{}^{16}O$ in ground and 1st excited bending vibrational-state," Chem. Phys. **31**, 19–29 (1978).
[94]T. Shimanouchi, *Tables of Molecular Vibrational Frequencies*, Consolidated Volume I (National Standard Reference Data Series, Gaithersburg, 1972), Vol. 39.
[95]M. Allan and T. Skalický, "Structures in elastic, vibrational, and dissociative electron attachment cross sections in N_2O near threshold," J. Phys. B: At., Mol. Opt. Phys. **36**, 3397–3409 (2003).
[96]S. P. McGlynn, J. W. Rabalais, J. R. McDonald, and V. M. Scherr, "Electronic spectoscopy of isoelectronic molecules. II. Linear triatomic groupings containing sixteen valence electrons," Chem. Rev. **71**, 73–108 (1971).
[97]R. I. Hall, A. Chutjian, and S. Trajmar, "Electron impact excitation and assignment of the low-lying electronic states of N_2O," J. Phys. B: At. Mol. Phys. **6**, L365–L368 (1973).
[98]D. F. Dance and I. C. Walker, "Electron energy loss spectrum of nitrous oxide," J. Chem. Soc., Faraday Trans. II **72**, 2105–2107 (1976).
[99]D. Cubric, D. Cvejanovic, J. Jureta, S. Cvejanovic, P. Hammond, G. C. King, and F. H. Read, "Threshold electron impact spectrum of N_2O," J. Phys. B: At. Mol. Phys. **19**, 4225–4239 (1986).
[100]S. E. Michelin, T. Kroin, and M. T. Lee, "Elastic and excitation cross sections for electron - nitrous oxide collisions," J. Phys. B: At., Mol. Opt. Phys. **29**, 2115–2125 (1996).
[101]H. Kawahara, D. Suzuki, H. Kato, M. Hoshino, H. Tanaka, O. Ingólfsson, L. Campbell, and M. J. Brunger, "Cross sections for electron impact excitation of the $C^1\Pi$ and $D^1\Sigma^+$ electronic states in N_2O," J. Chem. Phys. **131**, 114307 (2009).
[102]B. Marinkovic, R. Panajotovic, Z. Pesic, D. M Filipovic, Z. Felfli, and A. Z. Msezane, "Normalization of the measured relative electron differential cross sections for $2^1\Sigma^+$ and 1^Π states of N_2O," J. Phys. B: At., Mol. Opt. Phys. **32**, 1949–1957 (1999).
[103]M. Vinodkumar and M. Barot, "Scattering of N_2O on electron impact over an extensive energy range (0.1 eV–2000 eV)," J. Chem. Phys. **137**, 074311 (2012).
[104]T. Wróblewski, G. P. Karwasz, H. Nowakowska, J. Mechlińska-Drewko, V. T. Novaković, and Z. L. Petrović, "Semiempirical analysis of electron scattering cross sections in N_2O and CO_2," Czech J. Phys. **54**, C742 (2004).
[105]J. Mechlińska-Drewko, T. Wróblewski, Z. L. Petrović, V. Novaković, and G. P. Karwasz, "Electron scattering on N_2O-from cross sections to diffusion coefficients," Radiat. Phys. Chem. **68**, 205–209 (2003) [Proceedings of the 2nd Conference on Elementary Processess in Atomic Systems, CEPAS 2002, Gdansk, Poland, 2–6 September 2002].
[106]S. Dupljanin, J. de Urquijo, O. Šašić, E. Basurto, A. M. Juárez, J. L. Hernández-Ávila, S. Dujko, and Z. L. Petrović, "Transport coefficients and cross sections for electrons in N_2O and N_2O/N_2 mixtures," Plasma Sour. Sci. Tech. **19**, 025005 (2010).
[107]M. Hayashi (private communication, 1986).
[108]Y.-Y. Wang, J.-M. Sun, and L.-F. Zhu, "Cross sections for the valence shell excitations of nitrous oxide studied by fast electron impact," J. Chem. Phys. **132**, 124301 (2010).
[109]D. Rapp, P. Englander-Golden, and D. D. Briglia, "Cross sections for dissociative ionization of molecules by electron impact," J. Chem. Phys. **42**, 4081 –4085 (1965).
[110]B. Adamczyk, K. Bederski, L. Wójcik, and T. Stański, "Folio Scientatis Scientiarum Lublinensis Mat," Fiz. Chem. **18**, 217 (1976).
[111]H. A. van Sprang, G. R. Mohlmann, and F. J. De Heer, "Emission of radiation due to ionization and dissociation of N_2O by electron impact," Chem. Phys. **33**, 65–72 (1978).
[112]A. S. Newton and A. Sciamanna, "Metastable peaks in the mass spectra of N_2O and NO_2. II," J. Chem. Phys. **52**, 327–336 (1970).
[113]Computational Chemistry Comparison and Benchmark DataBase, "List of Experimental Polarizabilites," NIST (2018).
[114]E. Krishnakumar and S. K. Srivastava, "Dissociative attachment of electrons to N_2O," Phys. Rev. A **41**, 2445–2452 (1990).

[115]E. Krishnakumar (private communication, 2016).
[116]P. J. Chantry, "Temperature dependence of dissociative attachment in N_2O," J. Chem. Phys. **51**, 3369–3379 (1969).
[117]D. Nandi, V. S. Prabhudesai, and E. Krishnakumar, "Dissociative electron attachment to N_2O using velocity slice imaging," Phys. Chem. Chem. Phys. **16**, 3955–3963 (2014).
[118]C. Szmytkowski and P. Możejko, "Electron-scattering total cross sections for triatomic molecules: NO_2 and H_2O," Opt. Appl. **36**, 543 (2006).
[119]C. Szmytkowski, K. Maciag, and A. M. Krzysztofowicz, "NO_2 total absolute electron-scattering cross sections," Chem. Phys. Lett. **190**, 141–144 (1992).
[120]D. Gupta, R. Naghma, M. Vinodkumar, and B. Antony, "Electron scattering studies of nitrogen dioxide," J. Electron Spectrosc. Relat. Phenom. **191**, 71–78 (2013).
[121]D. Lukić, G. Josifov, and M. V. Kurepa, "Total electron-ionization cross sections of the NO_2 molecule," Int. J. Mass Spectrom. **205**, 1–6 (2001).
[122]K. N. Joshipura, S. Gangopadhyay, and B. G. Vaishnav, "Electron scattering and ionization of NO, N_2O, NO_2, NO_3 and N_2O_5 molecules: Theoretical cross sections," J. Phys. B: At., Mol. Opt. Phys. **40**, 199–210 (2007).
[123]H. Munjal, K. L. Baluja, and J. Tennyson, "Electron collisions with the NO_2 radical using the R-matrix method," Phys. Rev. A **79**, 032712 (2009).
[124]G. Herzberg, *Molecular Spectra and Molecular Structure. III: Electronic Spectra and Electronic Structure of Polyatomic Molecules* (Van Nostrand Reinhold, New York, 1966).
[125]S. Heitz, R. Lampka, D. Weidauer, and A. Hese, "Measurements of electric-dipole moments on NO_2," J. Chem. Phys. **94**, 2532–2535 (1991).
[126]S. Harrison, J. Tennyson, and A. Faure, "Calculated electron impact spin-coupled rotational cross sections for $^{2S+1}\Sigma^+$ linear molecules: CN as an example," J. Phys. B: At., Mol. Opt. Phys. **45**, 175202 (2012).
[127]J. W. Au and C. E. Brion, "Absolute oscillator strenghts for the valence-shell photoabsorption (2–200 eV) and the molecular and dissociative photoionization (11–80 eV) of nitrogen dioxide," Chem. Phys. **218**, 109–126 (1997).
[128]C. Q. Jiao, C. A. DeJoseph, and A. Garscadden, "Absolute cross sections for electron impact ionization of NO_2," J. Chem. Phys. **117**, 161–165 (2002).
[129]S. A. Rangwala, E. Krishnakumar, and S. V. K. Kumar, "Dissociative-electron-attachment cross sections: A comparative study of NO_2 and O_3," Phys. Rev. A **68**, 052710 (2003).
[130]R. Abouaf, R. Paineau, and F. Fiquet-Fayard, "Dissociative attachment in NO_2 and CO_2," J. Phys. B: At. Mol. Phys. **9**, 303–314 (1976).
[131]G. P. Karwasz, P. Możejko, and M.-Y. Song, "Electron-impact ionization of fluoromethanes—Review of experiments and binary-encounter models," Int. J. Mass Spectrom. **365-366**, 232–237 (2014), special issue: Tilmann Märk.
[132]D. A. Parkes and T. M. Sugden, "Electron attachment and detachment in nitric oxide," J. Chem. Soc., Faraday Trans. 2 **68**, 600–614 (1972).
[133]M. F. Skinker and J. V. White, "The motion of electrons in CO, N_2O and NO," Philos. Mag. Mag. **46**, 630–637 (1923).
[134]V. Bailey and J. Somerville, "The behaviour of electrons in Nitric Oxide," Philos. Mag. Mag. **17**, 1169–1176 (1934).
[135]C. S. Lakshminarasimha and J. Lucas, "The ratio of radial diffusion coefficient to mobility for electrons in helium, argon, air, methane and nitric oxide," J. Phys. D: Appl. Phys. **10**, 313–321 (1977).